GeoExpert ag

swiss*nuclear*: PEGASOS Refinement Project:
SP2 – Ground Motion Characterization

Contract no. PMT-VT-1032

Seismic Shear Wave Velocity Determination and Hybrid Seismic Survey at the SED-Station TORNY (Torny-le-Grand FR)

Date of Field Data Acquisition 6th April 2009

Report

Client

swiss*nuclear*
Project PRP
Frohburgstrasse 17
4601 Olten

Contractor

GeoExpert ag
Seismic Prospecting
Ifangstrasse 12b
P.O. Box 451
8603 Schwerzenbach

8603 Schwerzenbach, 20th May 2009

INDEX

1 INTRODUCTION

1.1 Survey objectives

The seismic survey's main task is to provide information about the distribution function of the shear wave velocities in the depth interval of the uppermost 30 m along a 100 m long seismic profile.

Additionally, the following objectives are to be met:

- the mapping of the topography of the rock face, i.e. the thickness of the Quaternary deposits;
- the determination of the thickness of the weathered zone and its degree of decompaction at the bedrock surface;
- a general view of geological structures.

1.2 The choice of the appropriate surveying methods

Several methods are available for deriving the s-wave velocity distribution in the subsurface at any given position:

- in-situ measurement by down-hole or crosshole seismic surveying;
- shear-wave refraction tomography profiling;
- dispersion analysis of surface waves (MASW; **M**ultiple channel **A**nalysis of **S**urface **W**aves)

The surveys are to be carried out at, or as close as possible near some 20 SED earth quake monitoring stations in Switzerland. Ideally, the surveys are to be conducted on two orthogonal profiles in order to derive at their point of intersection a robust 1D s-wave velocity distribution function by correlation. To this end, the methods of MASW and shear-wave refraction tomography profiling are to be combined.

The results are to include the following fundamental parameters $v_{s,5}$, $v_{s,10}$, $v_{s,20}$, $v_{s,30}$, $v_{s,40}$, $v_{s,50}$, $v_{s,100}$ are to be calculated, also an error estimation of all values.

The data acquired for the MASW method are to be subjected to complementary **p-wave hybrid seismic data processing** in order to image the geological structures.

Fig. 2.1: P-wave data acquisition at profile 09SN_17TORNY-P1.

2 FIELD DATA ACQUISITION PARTICULARS

2.1 Time Schedule

Date	*Time*	*Activities / remarks*
06.04.2009	1000	arrival from Schwerzenbach
	1000 - 1115	lay-out of recording spread profile 1
	1130 - 1200	compressional wave data recording profile 1
	1335 - 1410	shear wave data recording profile 1
	1410 - 1530	lay-out of recording spread profile 1 p-wave
	1530 - 1625	compressional wave data recording profile 1
	1630 - 1710	shear wave data recording profile 2
	1710 - 1800	retrieval of the recording spread
	1805	departure from site

2.2 Summary of Data Acquisition Parameters

Compressional Wave Data Acquisition

# of active channels	96
geophone type	4.5 Hz natural frequency, vertical velocimeter
receiver station spacing	1.0 m
# of geophones/station	1
source point spacing	2.0 m to 3.0 m
source type	vertical hammer (6 kg) striking on a horizontal metal plate
sampling rate	500 µs
recording time	2048 ms
field filters	0.5 Hz LC, anti-alias
# of field records	62 (line 09SN_17TORNY-P1) and 82 (line 09SN_17TORNY-P2)

Shear Wave Data Acquisition

# of active channels	48
geophone type	10 Hz natural frequency, horizontal velocimeter
receiver station spacing	2.0 m
# of geophones/station	1
source point spacing	4.0 m to 6.0 m
source type	horizontal hammer (6 kg) striking horizontally at a metal-plated wooden beam anchored to the ground by means of 20 cm long spikes
sampling rate	500 µs
recording time	512 ms
field filters	2 Hz LC, anti-alias
# of field records	50 at 25 positions (on both lines)

Fig. 2.2: S-wave data acquisition at profile 09SN_17TORNY-S2.

2.3 Composition of Seismic Field Crew

Personnel

Philippe Corboz	dipl. Natw. ETH Zurich, Geophysicist, party chief
Dieter Martin	Dipl.-Geolog, University of Freiburg I. Br., party chief
Kieron Lynch	assistant, spread lay-out and activation of seismic source

Equipment

96	vertical geophones 4.5 Hz
48	horizontal geophones 12 Hz
6	seismic cables
1	seismic acquisition system Summit Compact, 96 channels
1	laptop computer for data acquisition
3	walkie-talkies
1	hammer 6 kg
1	steel plate
1	metal-plated wooden beam
1	motorized barrow
1	van (FIAT Ducato 4x4)

2.4 Location

The seismic monitoring station TORNY (Torny-le-Grand FR) is situated on a loose moraine slope (some meters of thickness) overlaying Upper Marine Molasse in Swiss western midland basin, canton of Fribourg.

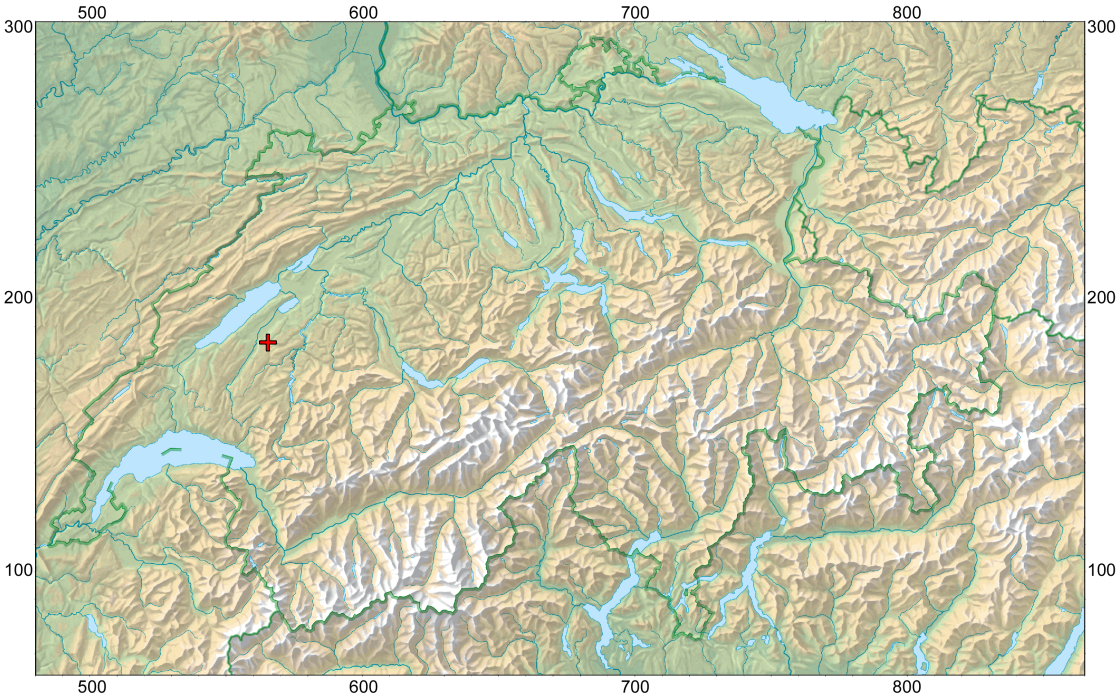

Fig. 2.3: The red cross marked seismic monitoring station TORNY (Torny-le-Grand FR) is located in Swiss western midland basin sediments (Upper Marine Molasse). (map: geodata @ swiss-topo).

2.5 Recording Conditions and Line Setup

The measurements could be done during sunny, warm and calm conditions.

In general, the seismic data quality and also the quality of surface wave content obtained at TORNY is to be rated as very high.

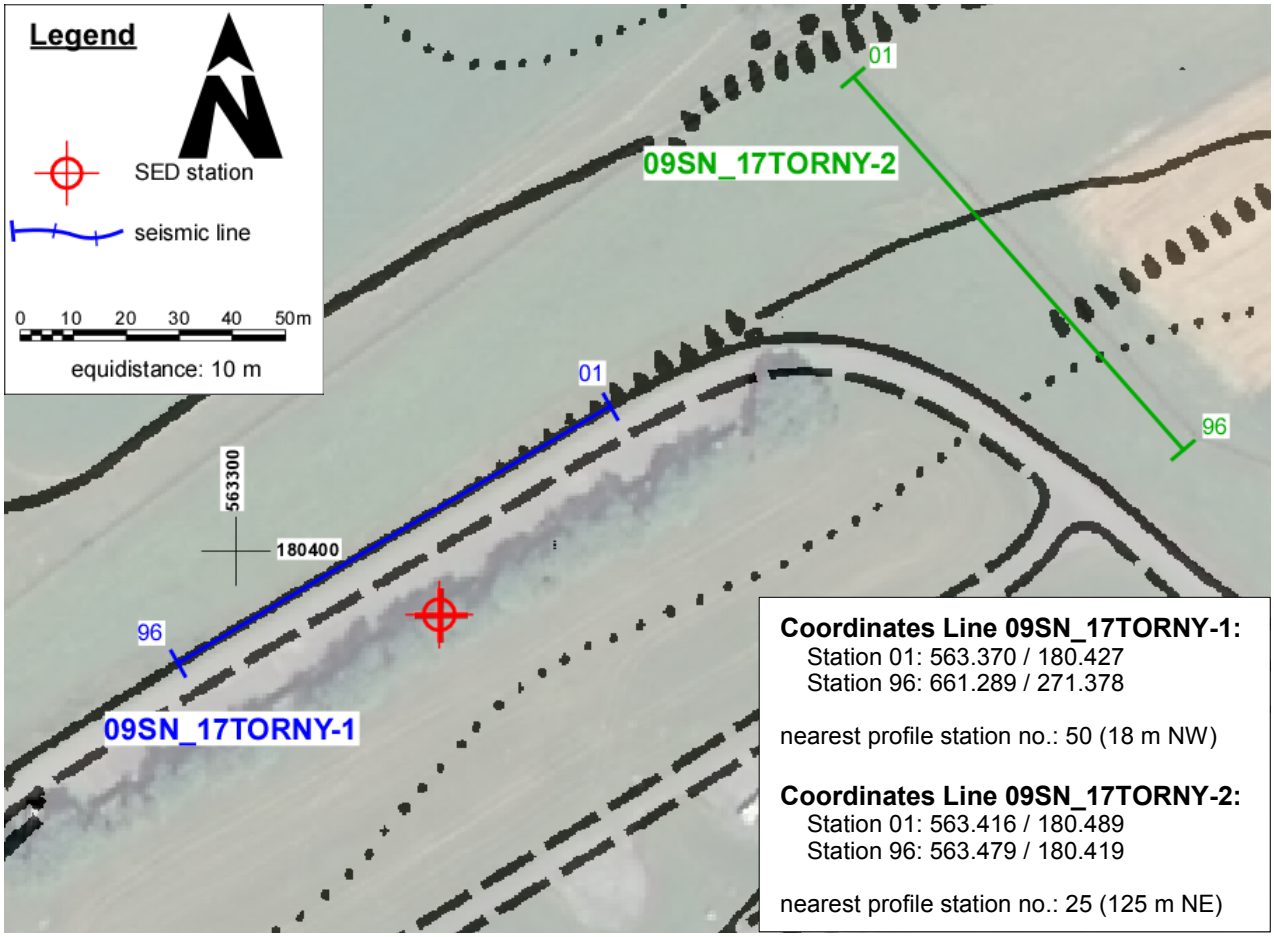

Fig. 2.4: Situation map with the trace of seismic profile 09SN_17TORNY-1 and -2. (background map: © State Fribourg.)

3 SEISMIC DATA PROCESSING AND IMAGING OF THE RESULTS

3.1 General Remarks

- For the shear and compressional wave refraction seismic evaluation the package **RAYFRACT** by Intelligent Resources Ltd., Vancouver CAN, was used. The system features the technique of diving wave tomography (www.rayfract.com).
- The system **SPW** (**S**eismic **P**rocessing **W**orkshop) of Parallel Geoscience Corporation, Austin US-TX, was used for reflection seismic data processing (www.parallelgeo.com).
- Data processing of surface waves (MASW processing) was conducted with the software package **SurfSeis** V2.0 of Kansas Geological Survey in Lawrence US-KS.

A detailed description of the various surveying methods will be included in the general summary report.

3.2 Shear Wave Refraction Tomography

3.2.1 Reformatting and field geometry assignment

After reformatting the field data into the Rayfract format the field geometry is applied.

3.2.2 First break time picking

At each shot position, two seismic records were acquired in both activation directions. These two records are displayed superimposed with different colors on each other in Fig 3.2a together with the manually determined first arrival time picks.

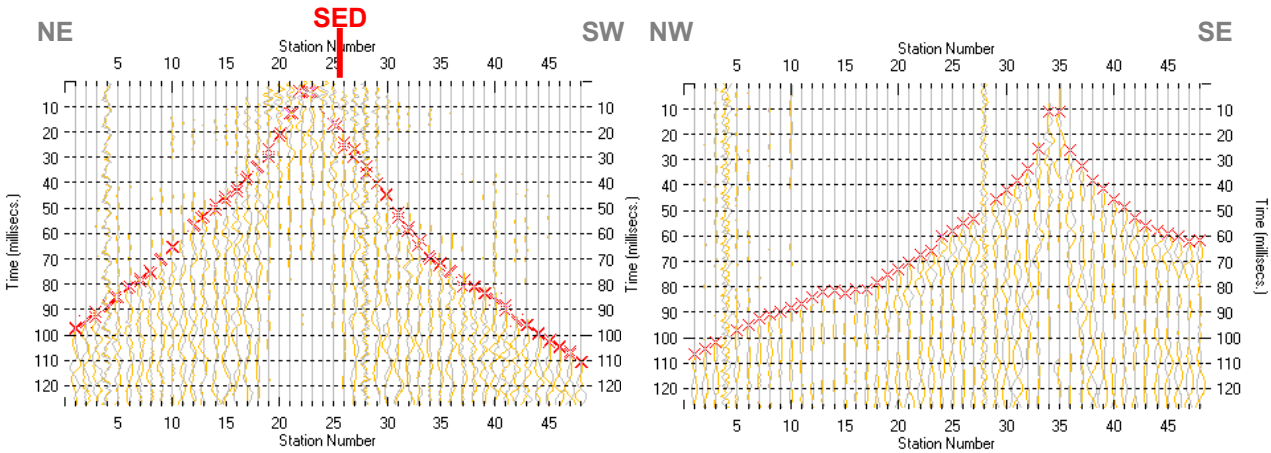

*Fig. 3.2a: High quality dual field record from line 09SN_17TORNY-S1 (left) and 09SN_17TORNY-S2 (right).showing at each station the s-wave traces with opposing polarities in different colors. The manually picked s-wave refraction arrivals at each station are marked with an **x**. The station spacing is 2 m, profile station number 00 = profile meter 0; profile station number 48 = profile meter 96.*

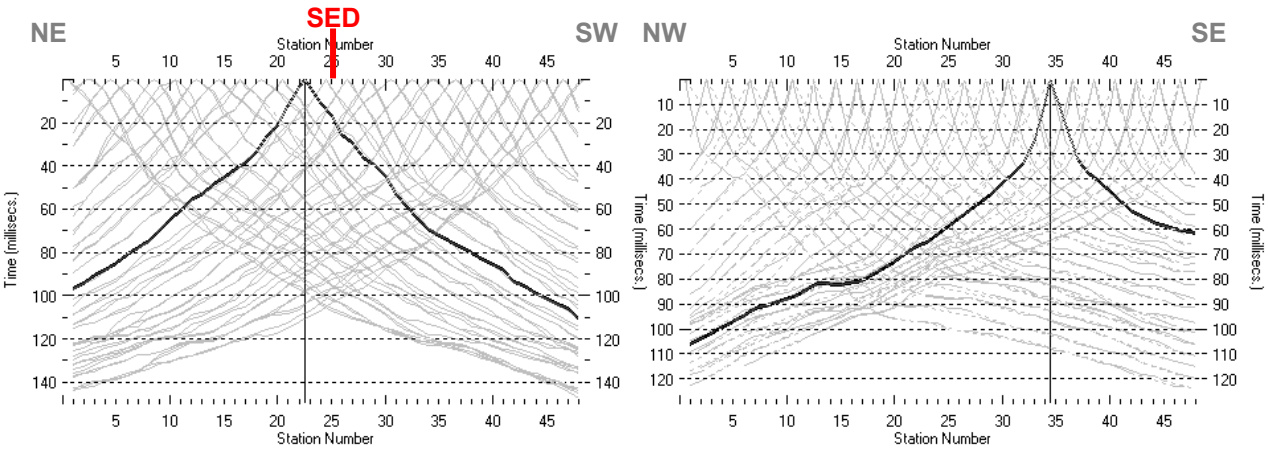

Fig. 3.2b: Curves of s-wave first break time picks from line 09SN_17TORNY-S1 (left) and -S2 (right).

3.2.3 Analytical Determination of Refraction Velocities

An initial 1D-velocity function (averaged 1D velocity-depth profiles derived by the Delta-t-V method, see Tab. 3.2a) is determined in the 3-dimensional time-offset-CMP-domain from all first break arrival time curves in the 3-dimensional time-offset-CMP-domain (see. Fig. 3.2c).

Depth [m]	Vs [m/s]
0.0	298
0.4	296
0.7	298
1.1	307
1.4	318
2.1	344
2.8	376
3.9	430
5.3	497
6.9	554
9.2	628
12.2	698
15.9	790
20.9	942
27.2	1195
35.7	1443
43.7	1719
49.9	1934

Depth [m]	Vs [m/s]
0.0	136
0.3	162
0.7	201
1.0	230
1.4	262
2.1	335
2.8	409
3.8	507
5.2	592
6.8	669
9.1	828
12.1	1055
15.7	1318
20.6	1503
26.9	1722
35.3	2252

Tab. 3.2a: Initial 1D s-wave velocity function derived from real data from line 09SN_17TORNY-S1 (mean values over the whole profile) and from line 09SN_17TORNY-S2.

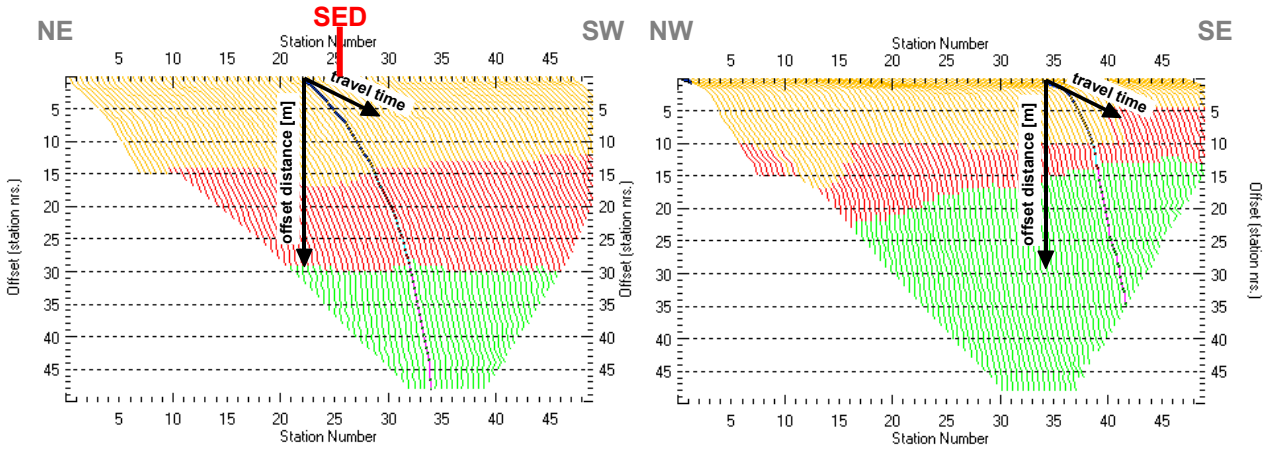

Fig. 3.2c: 3-dimensional distance-travel time diagrams from line 09SN_17TORNY-S1 (left) and 09SN_17TORNY-S2 (right) at the mid-points between source points and receiver stations are instrumental when using the analytical CMP derivation of the initial velocity field.
The horizontal axes are the along the CMP positions and the travel time respectively, the vertical axis denotes the offset distance between source and receiver positions. The colors represent different velocity layers. The station spacing is 2 m, profile station number 00 = profile meter 0; profile station number 48 = profile meter 96. The colors represent different velocity layers.

3.2.4 Tomographic inversion of the velocity gradient field by iterative modeling

The velocity field is iteratively refined by the subsequent Wavepath Eikonal Traveltime (WET) tomographic inversion process. The inversion results are portrayed in Fig. 3.2d as a gridded velocity contour section and in Fig. 3.2e as a ray path density section.

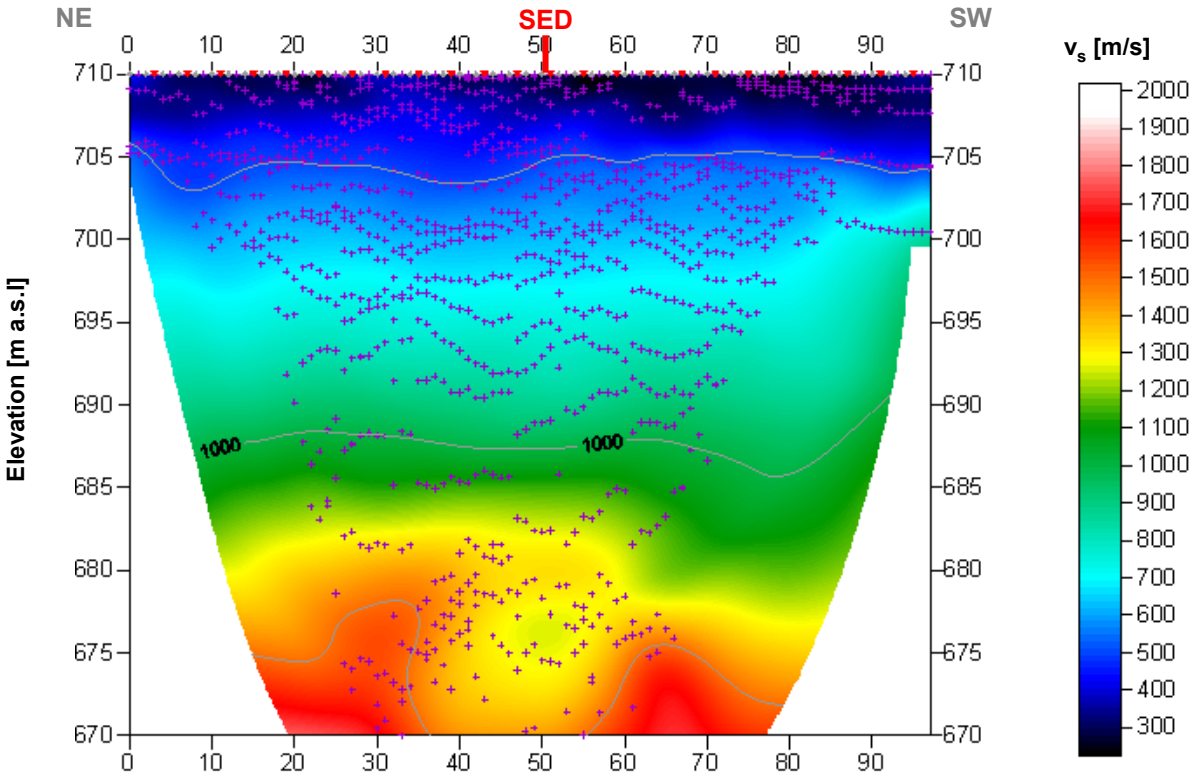

Fig. 3.2d: Shear wave velocity field of the line 09SN_17TORNY-S1. Red/white colors denote solid rock, blue/black colors point to unconsolidated sediments and soil.
Vertical axis: elevation [m a.s.l]; horizontal axis: profile meter; color encoded scale: v_s [m/s]; vertical exaggeration: 2:1; gray diamonds: receiver positions; red triangles: source positions; magenta crosses: positions of determined velocity values. The station spacing is 2 m, profile meter 0 = profile station number 00, profile meter 96 = profile station number 48.

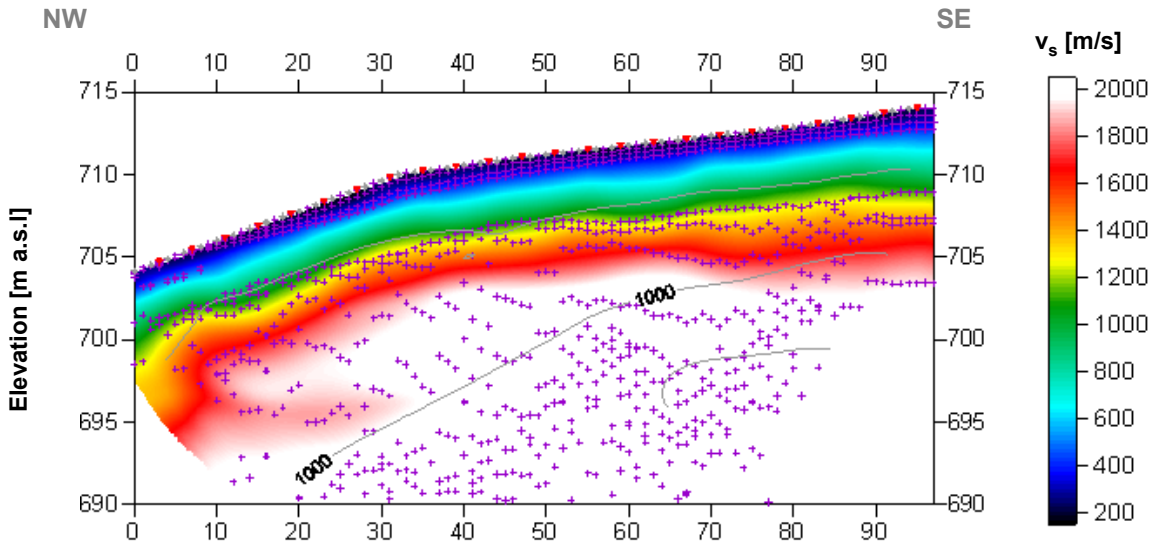

Fig. 3.2e: Shear wave velocity field of the line 09SN_17TORNY-S2. Red/white colors denote solid rock, blue/black colors point to unconsolidated sediments and soil.
Vertical axis: elevation [m a.s.l]; horizontal axis: profile meter; color encoded scale: v_s [m/s]; vertical exaggeration: 2:1; gray diamonds: receiver positions; red triangles: source positions; magenta crosses: positions of determined velocity values. The station spacing is 2 m, profile meter 0 = profile station number 00, profile meter 96 = profile station number 48.

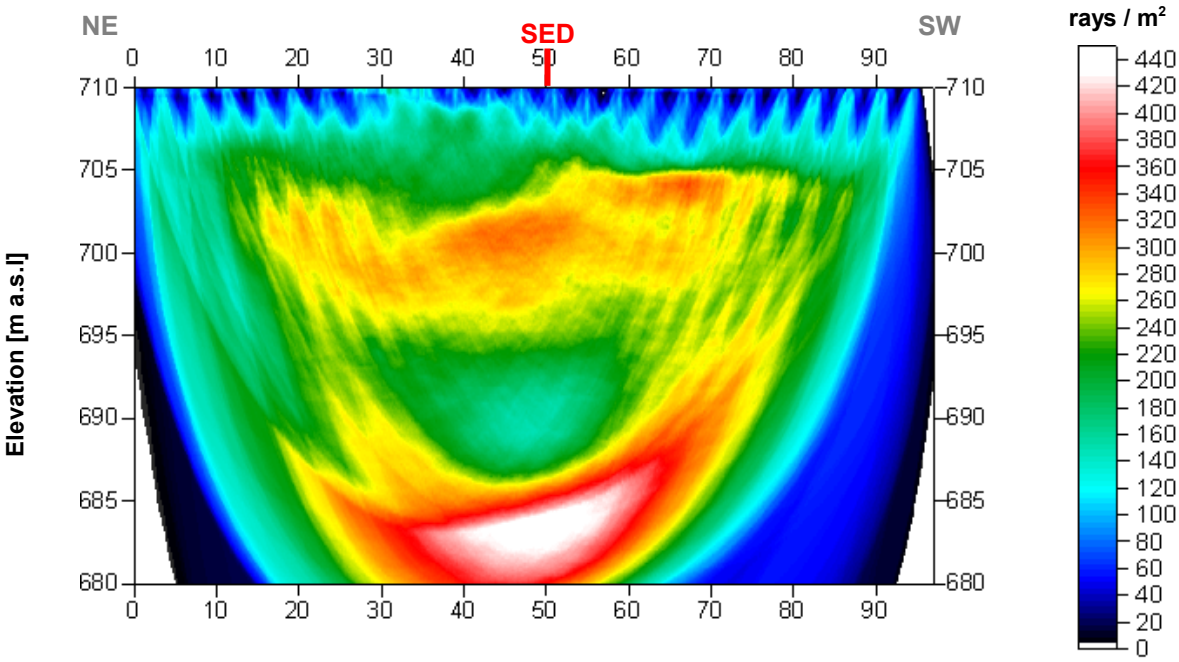

Fig. 3.2f: Shear wave ray path density along the seismic line 09SN_17TORNY-S1. Red/white colors indicate high velocity contrasts (usually at the bedrock surface), blue/black colors denote low coverage areas. Vertical axis: elevation [m a.s.l]; horizontal axis: profile meter; color encoded scale: ray paths per m²; vertical exaggeration: 2:1. The station spacing is 2 m, profile meter 0 = profile station 00, profile meter 96 = profile station 48.

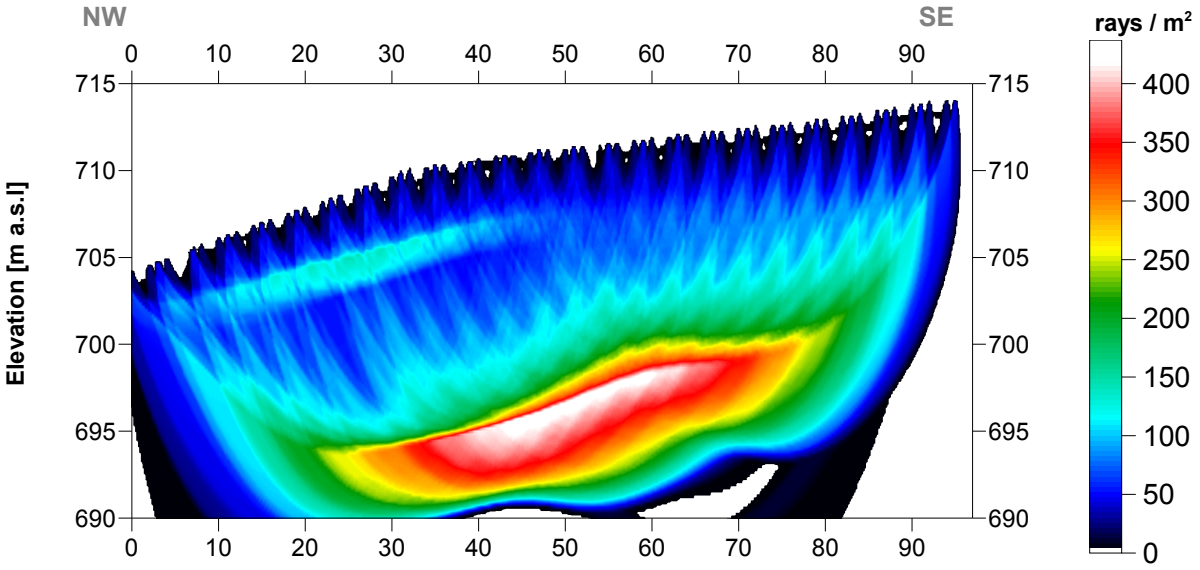

Fig. 3.2g: Shear wave ray path density along the seismic line 09SN_17TORNY-S2. Red/white colors indicate high velocity contrasts (usually at the bedrock surface), blue/black colors denote low coverage areas. Vertical axis: elevation [m a.s.l]; horizontal axis: profile meter; color encoded scale: ray paths per m²; vertical exaggeration: 2:1. The station spacing is 2 m, profile meter 0 = profile station 00, profile meter 96 = profile station 48.

Depth [m]	Vs [m/s]
0.0	394
2.1	244
4.3	362
6.4	564
8.5	741
10.6	860
12.8	943
14.7	943
16.8	955
18.9	961
21.1	992
23.2	1036
25.3	1097
27.5	1170
29.4	1208
31.5	1254
33.6	1303
35.8	1361
37.9	1400
40.0	1449
42.0	1495

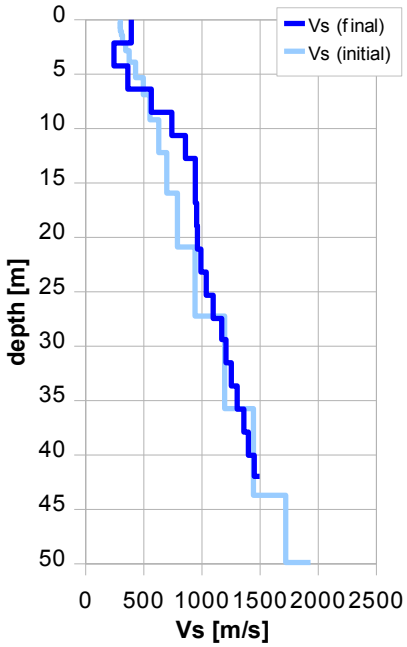

Tab. 3.2b: Final 1D s-wave velocity model derived from real data from line 09SN_17TORNY-S1 (horizontal average of all values). The calculated values of the initial 1D s-wave velocity model are given in Tab. 3.2a.

Depth [m]	Vs [m/s]
0.0	122
1.0	220
2.1	353
3.1	471
4.2	554
5.2	601
6.3	644
7.3	701
8.4	773
9.4	856
10.5	938
11.5	1022
12.6	1108
13.6	1188
14.7	1255
15.7	1309
16.6	1258
17.7	1239

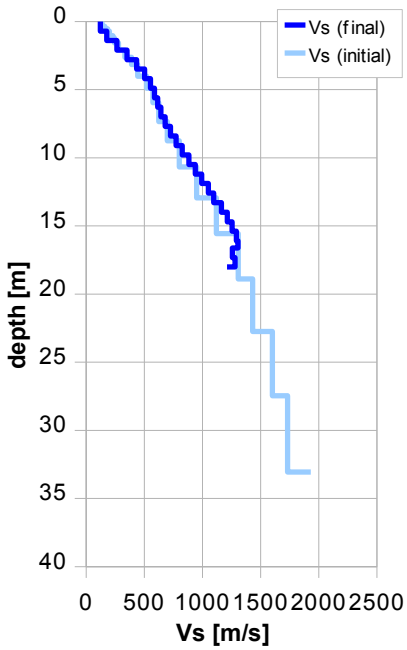

Tab. 3.2c: Final 1D s-wave velocity model derived from real data from line 09SN_17TORNY-S2 (horizontal average of all values). The calculated values of the initial 1D s-wave velocity model are given in Tab. 3.2a.

3.3 MASW Processing

3.3.1 Reformatting and field geometry assignment

The data preparation steps for the dispersion analysis include

- the assignment of the field acquisition geometry
- the selection of suitable offset ranges (=arrays) between 10 m and 50 m for dispersion, and the splitting of the field records in forward and reverse shooting direction data sets
- the reformatting of the data into the specific KGS format

X - - ... - - o-o-o-...-o-o-o (forward shooting or so-called PLUS direction)
respectively
o-o-o-...-o-o-o - - ... - - X (reverse shooting or so-called MINUS direction).

where **X** = shot position
o = receiver station
- = 1.0 m offset

The active array used at SED-station TORNY are the receiver station in the shot offset range between 10 and 50 m. An additional analysis was done with 20 to 105 m arrays.

3.3.2 Calculating the dispersion image (overtone)

The result of dispersion analysis is the color encoded acoustic energy distribution in the phase velocity - frequency plane (see Fig. 3.3a, b and c).

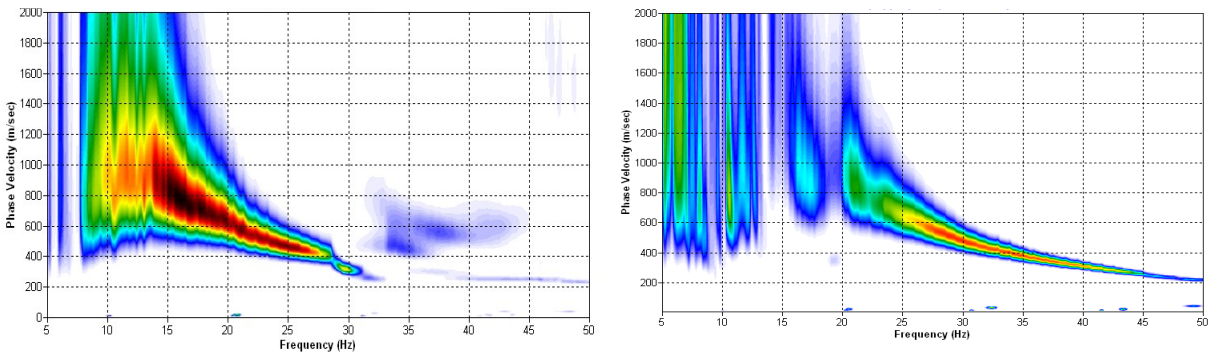

Fig. 3.3a: Dispersion image of high quality data (left) from midpoint station 66 (line 09SN_17TORNY-M1) as found on 90 % and of fair quality data (right) from midpoint station 68 (line 09SN_17T-ORNY-M2) representing about 10 % of the MASW dataset of site TORNY.
Horizontal axis: frequency from 5 to 50 Hz; vertical axis: phase velocity from 0 to 2000 m/s; color code: colors from white (no energy) to blue - green - yellow - red - black point to increasing energy amplitude values.

3.3.3 Analysis of the dispersion image

In the dispersion graphs as calculated in section 3.3.2 above, the curves joining the amplitude peaks of the fundamental modes are determined either by subjective inspection or in a semi-automated manner. On datasets with poorly defined amplitude peaks or with a highly irregular alignment of the peaks, the danger of obtaining improbable or wrong results is real and can only be mitigated by the processing experience and the a-priori knowledge of the geological setting by the geophysicist responsible for the data evaluation.

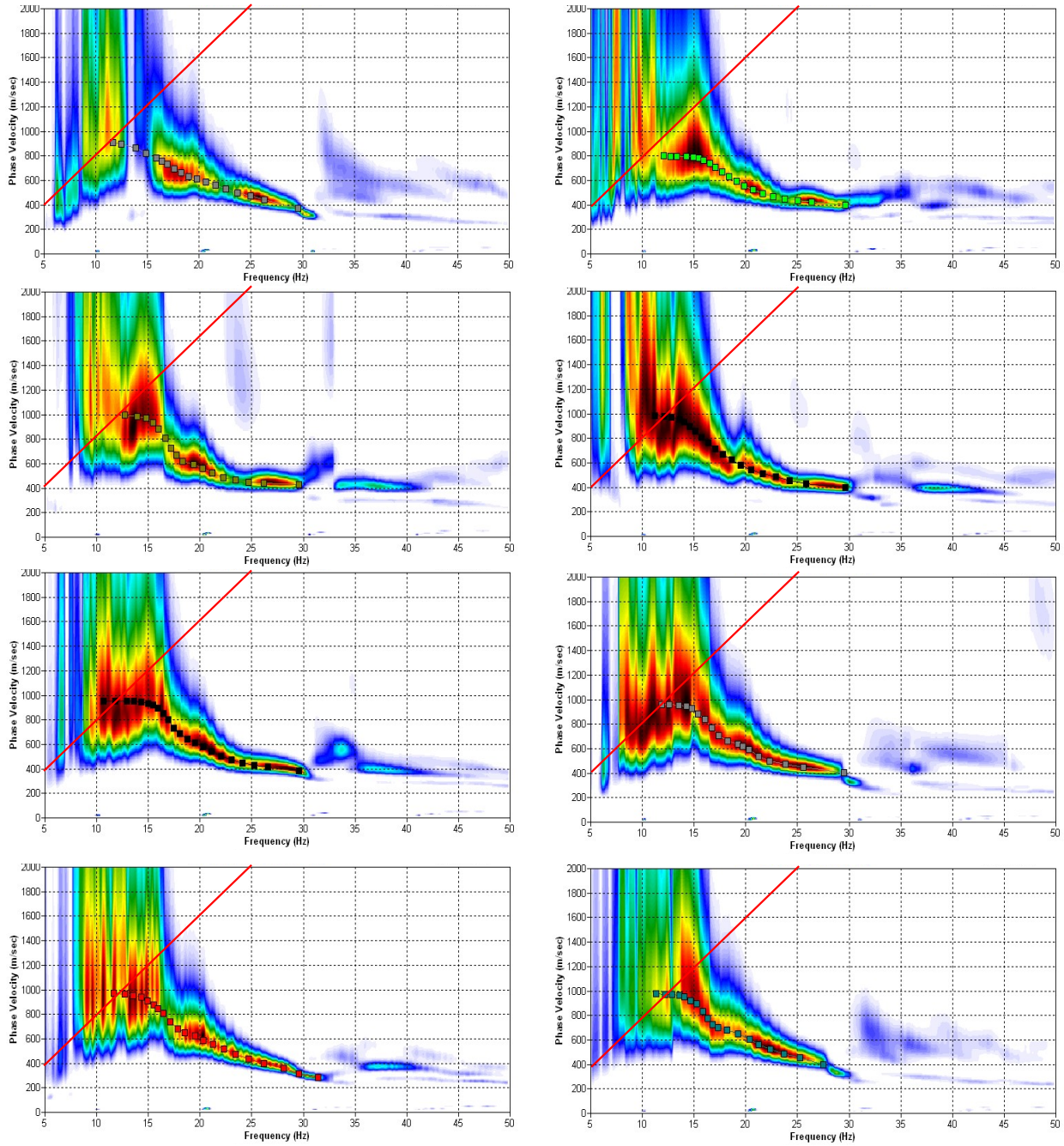

Fig. 3.3b: The manually picked dispersion images used for the derivation of the shear wave velocity section on line 09SN_17TORNY-M1. The dispersion curves (squares) are determined by linking the peaks of high energy. Note that 'higher modes' may at times produce higher energy peaks than the fundamental mode required for the analysis.
dotted fine line: signal-noise ratio for the designated f-v_{ph} – value.
red line: high resolution beam-forming curve for v_{max}.
1st row: left: station 23 @ PLUS direction; right: station 22 @ MINUS direction
2nd row: left: station 39 @ PLUS direction; right: station 38 @ MINUS direction
3rd row: left: station 55 @ PLUS direction; right: station 58 @ MINUS direction
4th row: left: station 77 @ PLUS direction; right: station 74 @ MINUS direction

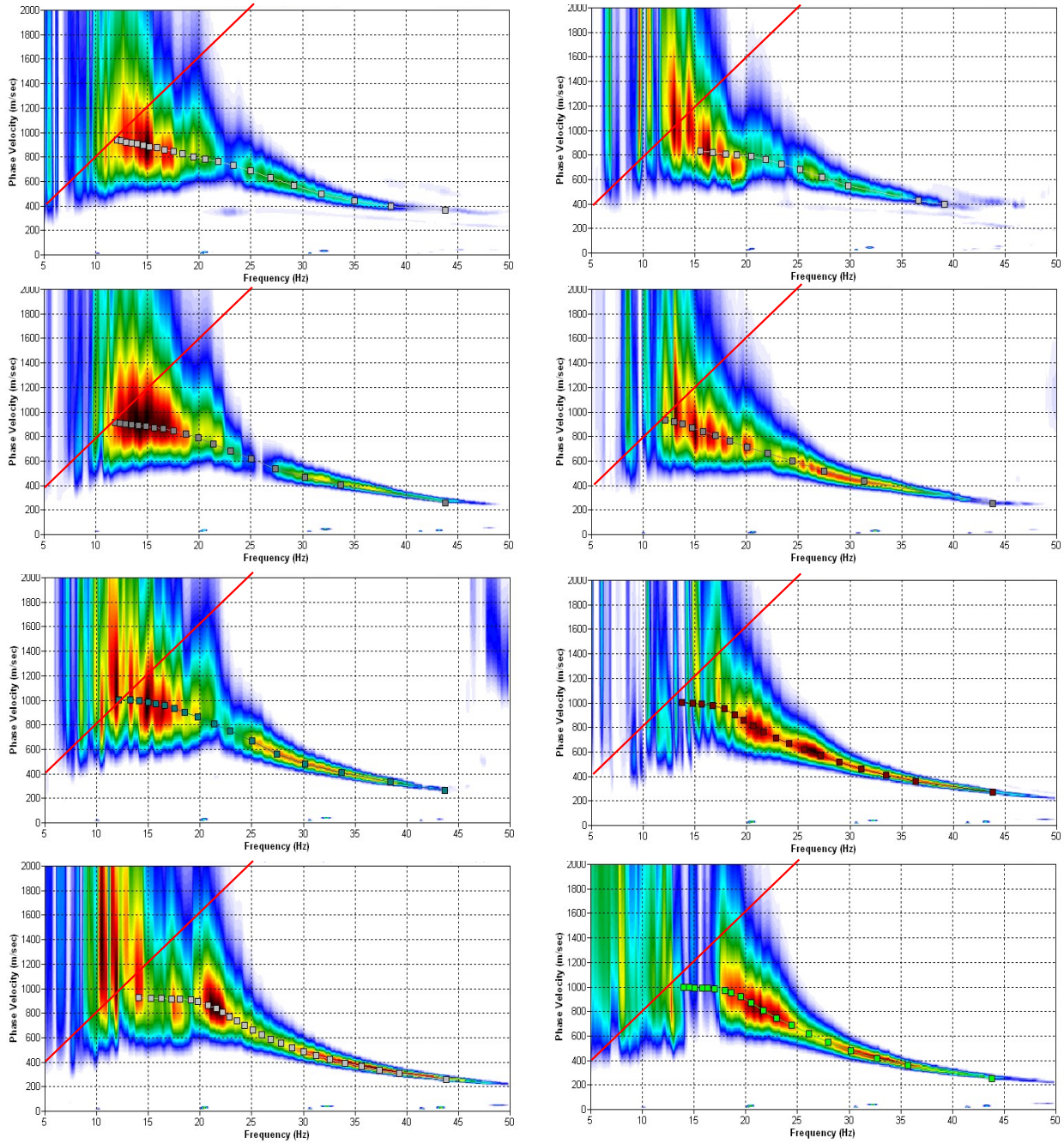

Fig. 3.3c: The manually picked dispersion images used for the derivation of the shear wave velocity section on line 09SN_17TORNY-M2. The dispersion curves (squares) are determined by linking the peaks of high energy. Note that 'higher modes' may at times produce higher energy peaks than the fundamental mode required for the analysis.
dotted fine line: signal-noise ratio for the designated f-v_{ph} – value.
red line: high resolution beam-forming curve for v_{max}.
1st row: left: station 27 @ PLUS direction; right: station 22 @ MINUS direction
2nd row: left: station 41 @ PLUS direction; right: station 40 @ MINUS direction
3rd row: left: station 61 @ PLUS direction; right: station 60 @ MINUS direction
4th row: left: station 78 @ PLUS direction; right: station 76 @ MINUS direction

3.3.4 Inversion of dispersion curves resulting in a 1D shear wave velocity distribution

Inversion of the extracted dispersion curves was performed using the algorithm described by Xia et al. (1999).

The inversion process is started by setting the maximum depth (z_{max}) to be in the order of 30% of the largest wavelength for an initial model consisting of 10 layers of increasing thicknesses. For all 10 layers the Poisson's ratio is assumed to be 0.4 and the rock/soil density to be 2.0 g/cm^3. The inversion process is concluded either after twelve iterations or when the convergence condition of a RMS-error of less than 3 m/s (phase velocity) is met.

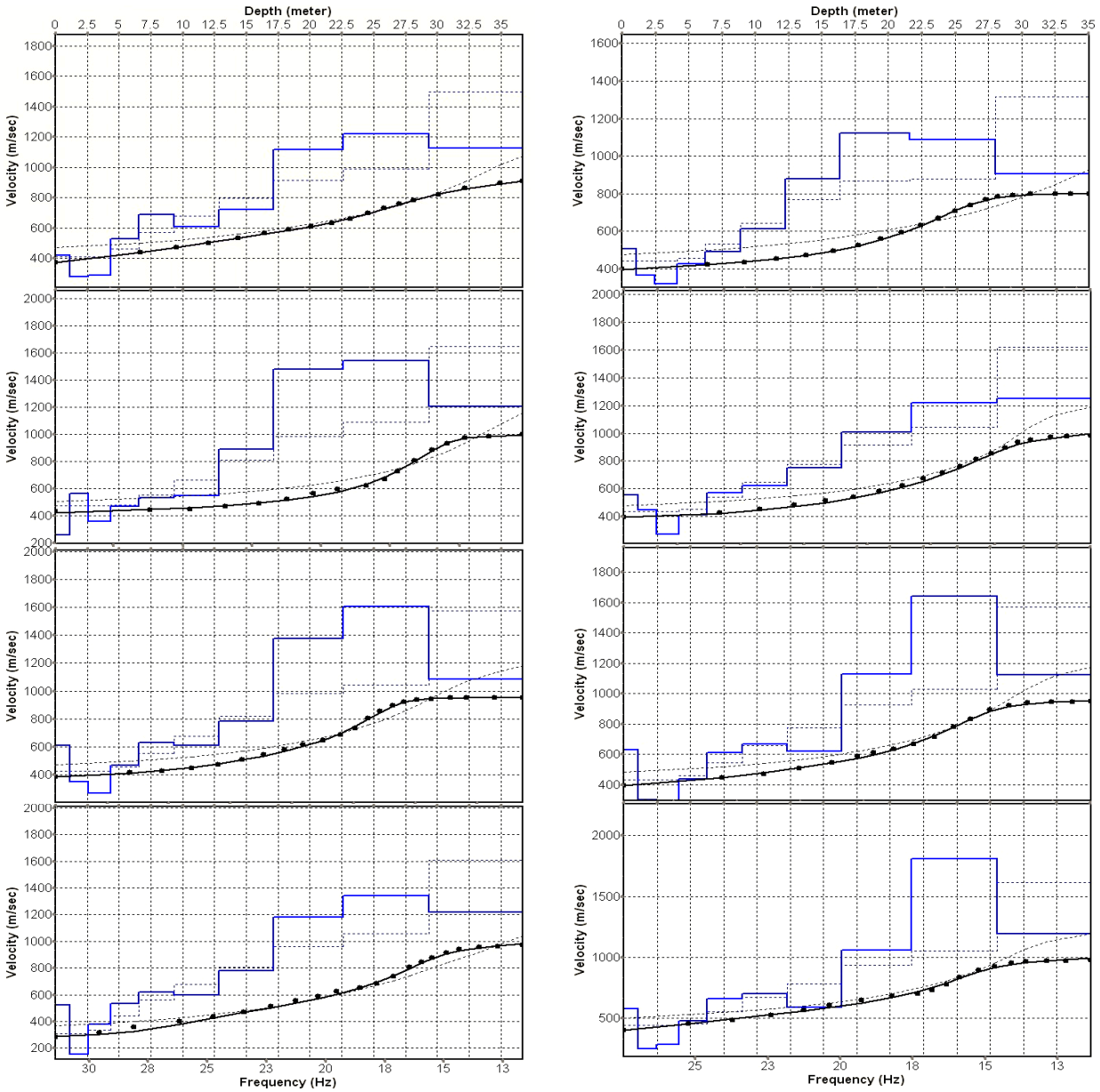

Fig. 3.3d: Inversion results of dispersion curves from dataset at line 09SN_17TORNY-M1.
***brown**: Inversion of dispersion curve (dots) resp. of the modeled dispersion curve (dotted line: initial model; continuous line: end model). Horizontal axis: frequency Hz, vertical axis: v_s.*
***blue**: 10-layer-model (dotted: initial model, continuous line: final model). Horizontal axis: depth, vertical axis: phase velocity resp. v_s).*
1st row: left: station 23 @ PLUS direction; right: station 22 @ MINUS direction
2nd row: left: station 39 @ PLUS direction; right: station 38 @ MINUS direction
3rd row: left: station 55 @ PLUS direction; right: station 58 @ MINUS direction
4th row: left: station 77 @ PLUS direction; right: station 74 @ MINUS direction

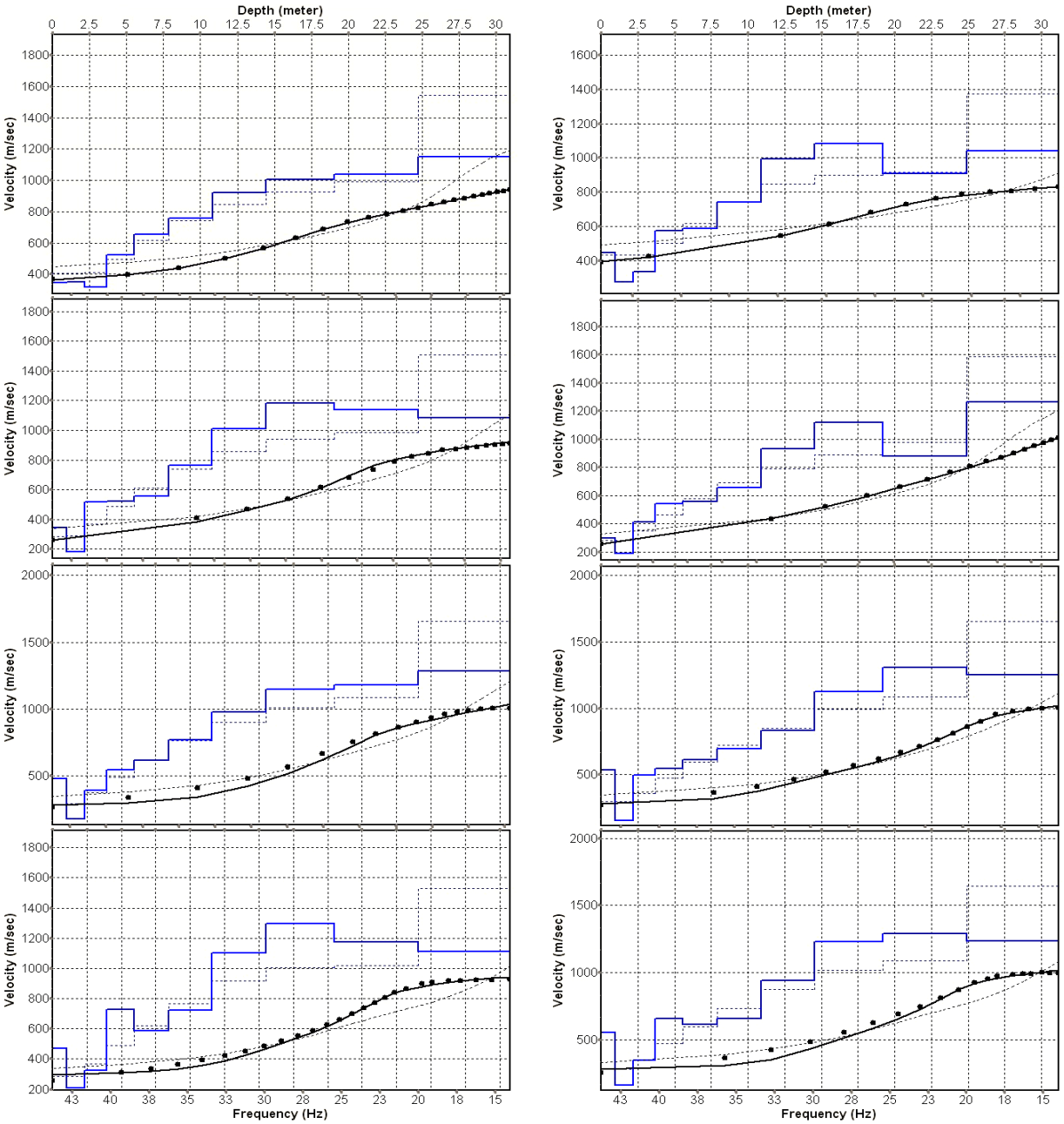

Fig. 3.3e: Inversion results of dispersion curves from dataset at line 09SN_17TORNY-M2.
***brown**: Inversion of dispersion curve (dots) resp. of the modeled dispersion curve (dotted line: initial model; continuous line: end model). Horizontal axis: frequency Hz, vertical axis: v_s.*
***blue**: 10-layer-model (dotted: initial model, continuous line: final model). Horizontal axis: depth, vertical axis: phase velocity resp. v_S).*
1st row: left: station 27 @ PLUS direction; right: station 22 @ MINUS direction
2nd row: left: station 41 @ PLUS direction; right: station 40 @ MINUS direction
3rd row: left: station 61 @ PLUS direction; right: station 60 @ MINUS direction
4th row: left: station 78 @ PLUS direction; right: station 76 @ MINUS direction

Dispersion analyses of records with longer receiver arrays should – by theory – increase the investigation depth. At TORNY, with both lines and both directions, MASW processing with the maximal array length of 95 m doesn't improve the results (Fig. 3.3f and 3.3g).

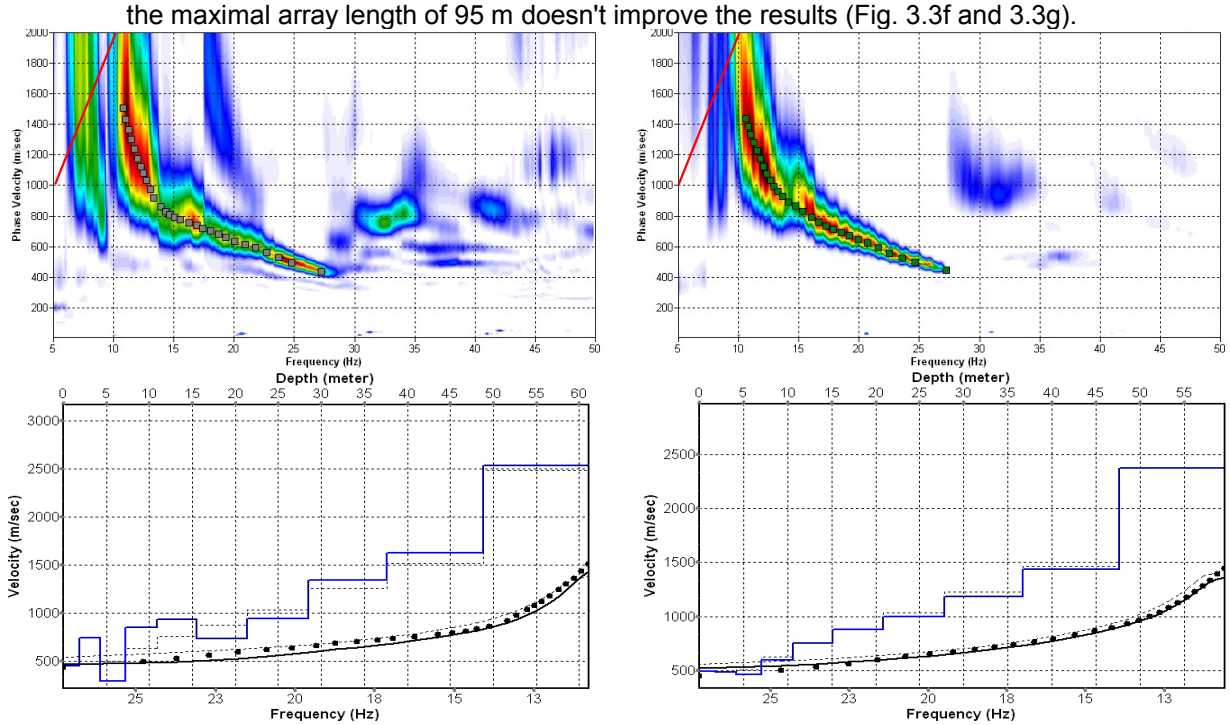

Fig. 3.3f: Top: dispersion images of over-all arrays (20...116 m offset) from line 09SN_17TORNY-M1 in PLUS (left) and MINUS (right) direction; dotted fine line: signal-noise ratio for the designated f-v_{ph}-value. Red line: high resolution beam-forming curve for v_{max}.
*Below: The two respective inversion results; **brown**: inversion of dispersion curve; **blue**: 10-layer-model. Horizontal axis: depth, vertical axis: phase velocity resp. v_s.*

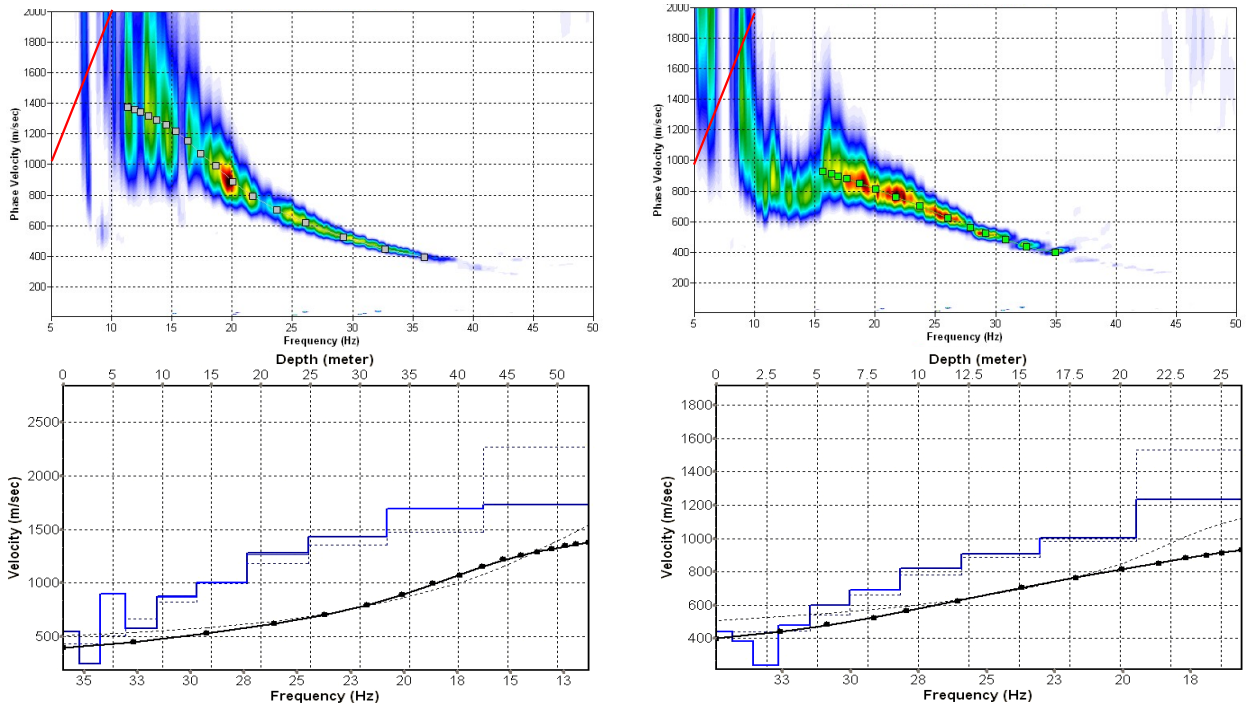

Fig. 3.3g: Top: dispersion images of over-all arrays (20...116 m offset) from line 09SN_17TORNY-M2 in PLUS (left) and MINUS (right) direction; dotted fine line: signal-noise ratio for the designated f-v_{ph} – value. Red line: high resolution beam-forming curve for v_{max}.
*Below: The two respective inversion results; **brown**: inversion of dispersion curve; **blue**: 10-layer-model. Horizontal axis: depth, vertical axis: phase velocity resp. v_s.*

3.3.5 Gridding and plotting of 2D v_s-velocity field

By assembling the 1D v_s - depth functions from all stations the final 2D v_s-field is derived using a Kriging gridding procedure as portrayed in Fig. 3.3h and 3.3i below:

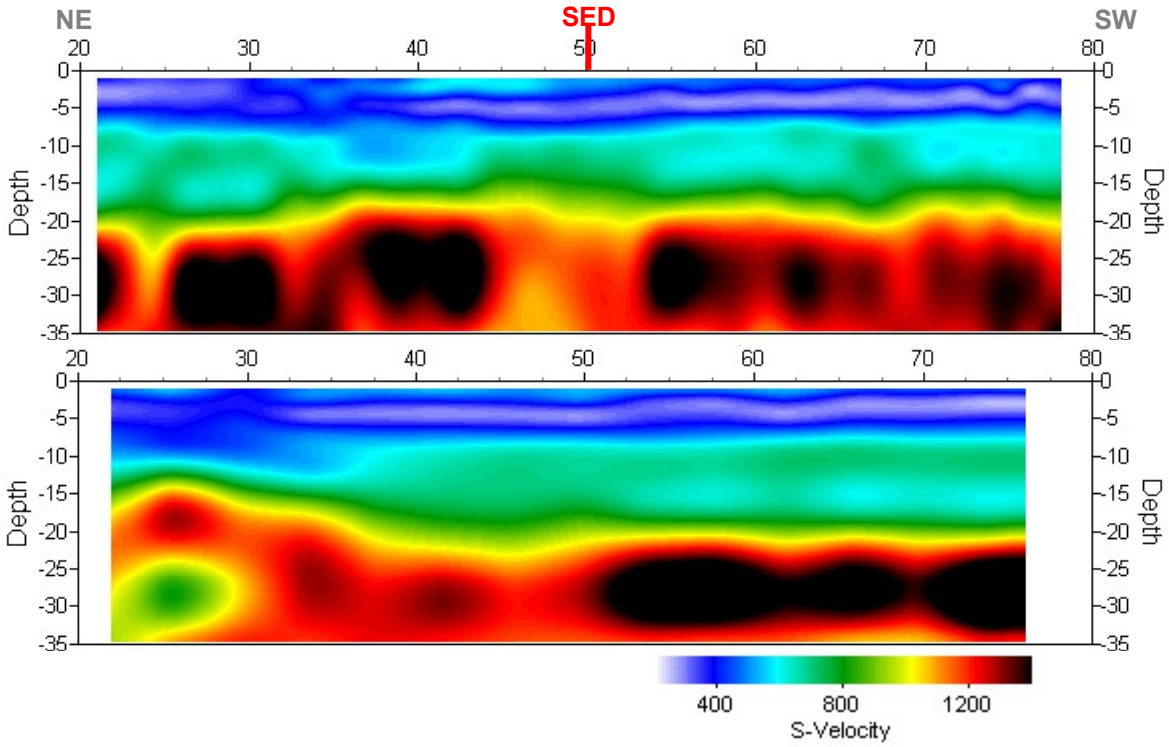

Fig. 3.3h: PLUS- (above) and MINUS- (below)-MASW-processed shear wave velocity fields from line 09SN_17TORNY-M1. Station spacing is 1 m.

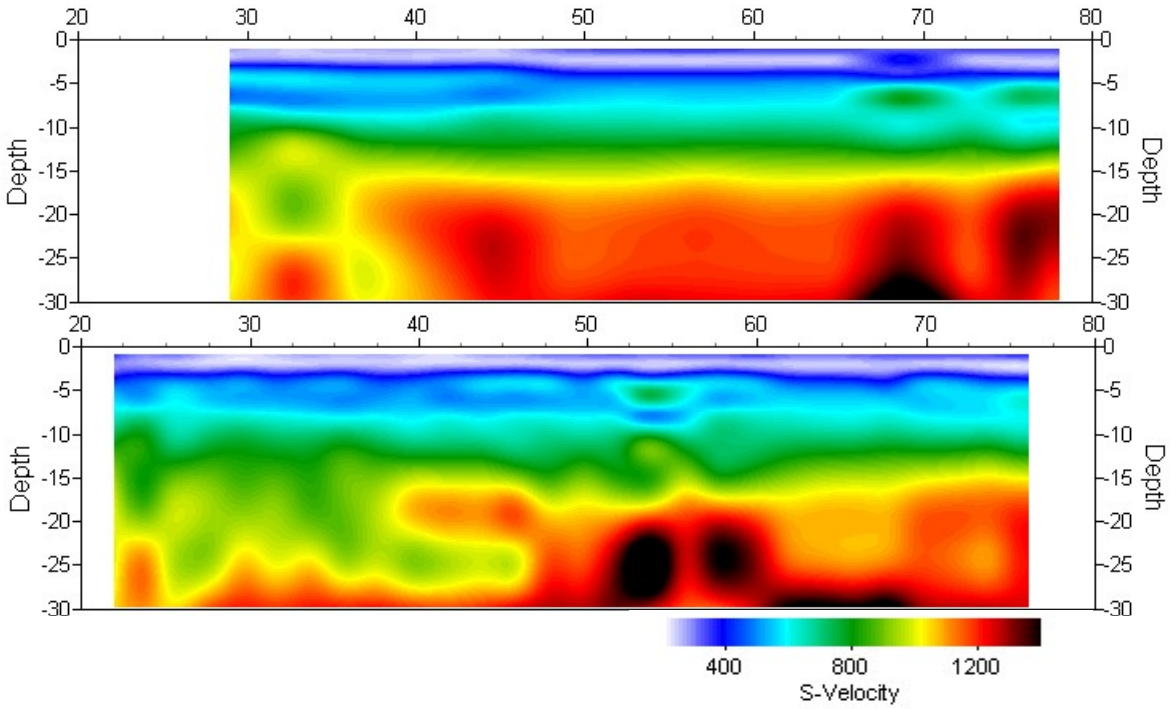

Fig. 3.3i: PLUS- (above) and MINUS- (below)-MASW-processed shear wave velocity fields from line 09SN_17TORNY-M2. Station spacing is 1 m.

3.3.6 Calculation of the average shear wave velocity

In order to calculate a representative shear wave velocity-depth function from line 09SN_17TORNY-M1 at the SED station, all computed 1D-v_S-depth functions – are averaged (non-weighted mean values). The v_S-depth-function is shown in Tab. 3.3a.

Depth [m]	Vs+ [m/s]	Vs- [m/s]	Vs [m/s]
1.1	560	467	514
2.5	391	424	408
4.2	293	299	296
6.4	430	466	448
9.1	588	610	599
12.5	668	644	656
16.8	756	822	789
22.1	1078	1190	1134
28.7	1355	1341	1348
35.9	1133	1216	1174

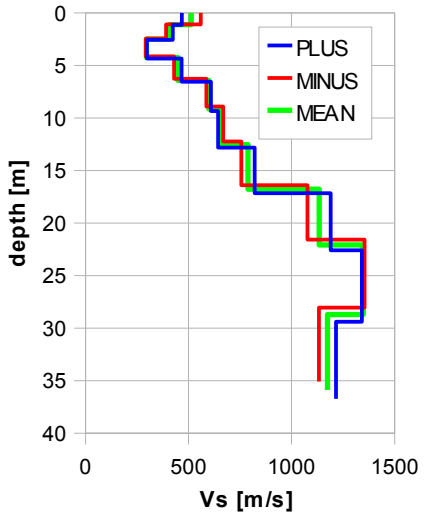

Tab. 3.3a: Averaged vs - depth function from line 09SN_17TORNY-M1 at the SED station. Blue line: MASW-'PLUS' processing, red line: MASW-'MINUS' processing; green line: average of PLUS- and MINUS-functions.

In order to calculate an representative shear wave velocity-depth function from line 09SN_17TORNY-M2 at the SED station, all computed 1D-v_S-depth functions are averaged (non-weighted mean values). The resulting v_S-depth-function is shown in Tab. 3.3b.

Depth [m]	Vs- [m/s]	Vs+ [m/s]	Vs [m/s]
1.0	400	397	399
2.2	182	212	197
3.1	441	425	433
5.8	544	578	561
8.2	578	604	591
11.2	722	764	743
15.1	883	998	941
19.8	1060	1162	1111
25.8	1111	1177	1144
32.2	1274	1256	1265

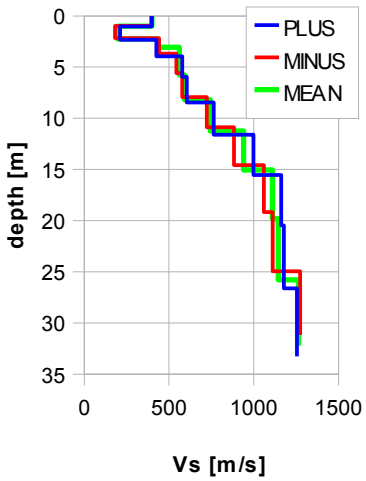

Tab. 3.3b: Averaged v_S - depth function from line 09SN_17TORNY-M2 at the SED station (ca. 120 m offset from line). Blue line: MASW-'PLUS' processing, red line: MASW-'MINUS' processing; green line: average of PLUS- and MINUS-functions.

The inversion of the four 100 m-array dispersion curves data (20 to 116 m offset, see Fig. 3.3f and 3.3g) are given in Tab. 3.3c. These values are complemented with the values derived from the 40 m-arrays analyses (Tab. 3.3a and 3.3b).

	100 m array							40 m array			
depth	m1+	m1-	m2+	m2-	m1	m2	m	depth	m1	m2	m
1.6	452	491	545	(438)*	471	463	496	1.1	514	399	456
3.5	743	486	247	(381)*	614	243	492	2.4	408	197	302
5.9	290	460	896	(239)*	375	746	548	3.6	296	433	364
8.9	849	592	577	(476)*	720	633	672	6.1	448	561	505
12.7	932	753	872	(597)*	843	847	852	8.7	599	591	595
17.5	737	878	1001	(688)*	808	1002	872	11.9	656	743	700
23.4	943	999	1280	(821)*	971	1256	1074	15.9	789	941	865
30.8	1346	1183	1430	(905)*	1264	1430	1320	21.0	1134	1111	1122
40.0	1629	1435	1689	(1004)*	1532	1689	1585	27.2	1348	1144	1246
50.0	2535	2372	1727	(1232)*	2454	1727	2211	34.1	1174	1265	1220

Tab. 3.3c: *v_S-depth values from the four MASW-derived dispersion curves of both seismic line 09SN_17TORNY-M1 and 09SN_17TORNY-M2 using 100 m-arrays. The dispersion curves are shown in Fig. 3.3f and Fig 3.3g.*
**The belonging depths to the vs-values from analysis of m2-data are from 0.8 to 26 m.*

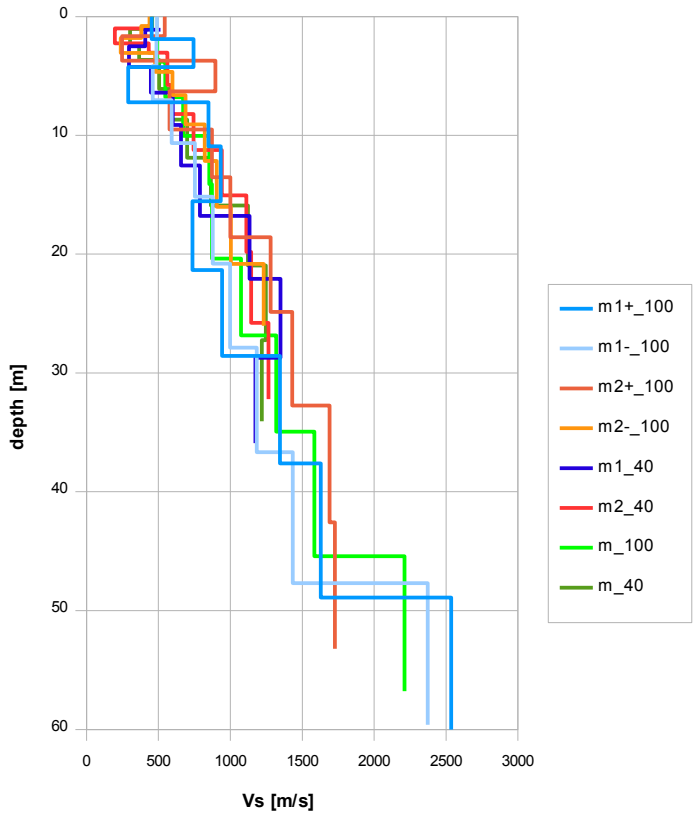

Fig. 3.3j: *Comparison of the ensemble of inversion results of both lines 09SN_17TORNY-M1 and -M2, either using the 40 m- and the 100 m-arrays.*
blue lines: analyses of records from line 09SN_17TORNY-M1
red lines: analyses of records from line 09SN_17TORNY-M2
light green line: mean of both 100 m-array records analyses in MINUS and PLUS direction.
dark green line: mean v_S-value from analyses of 40 m-array records.

3.3.7 Calculation of the shear wave velocity scalars $v_{s,5}$, $v_{s,10}$, ...

The parameters $v_{s,5}$, $v_{s,10}$, $v_{s,20}$, $v_{s,30}$, $v_{s,40}$, $v_{s,50}$ represent the average shear wave velocities in the depth interval between the surface and the respective depth levels and are determined from the formula

$$v_{s,n} = \frac{\sum_{i=1}^{n} d_i}{\sum_{i=1}^{n} d_i / v_{si}}$$

with:

d_i = thickness of layer i
v_{si} = corresponding shear-wave velocity.

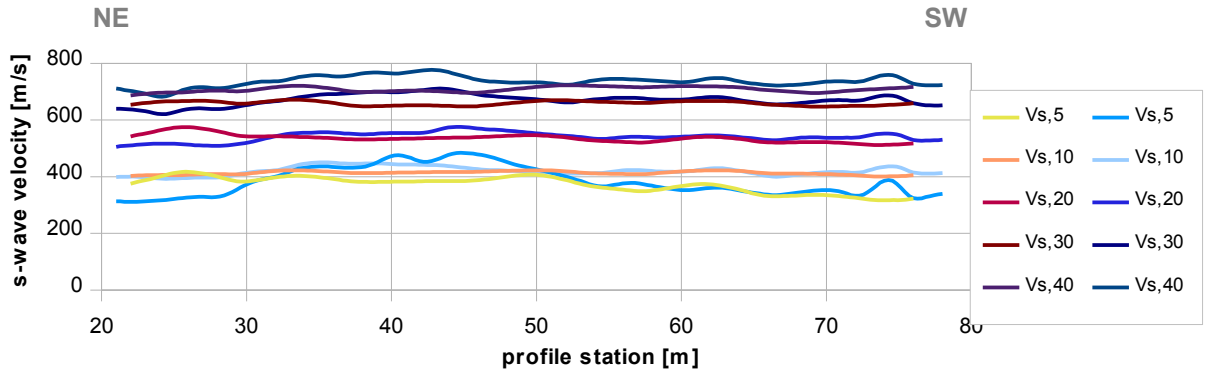

Fig. 3.3k: Graphs of the averaged vs,5...-values along the line 09SN_17TORNY-M1 for the PLUS- (blue lines) and MINUS- (red lines) directions.

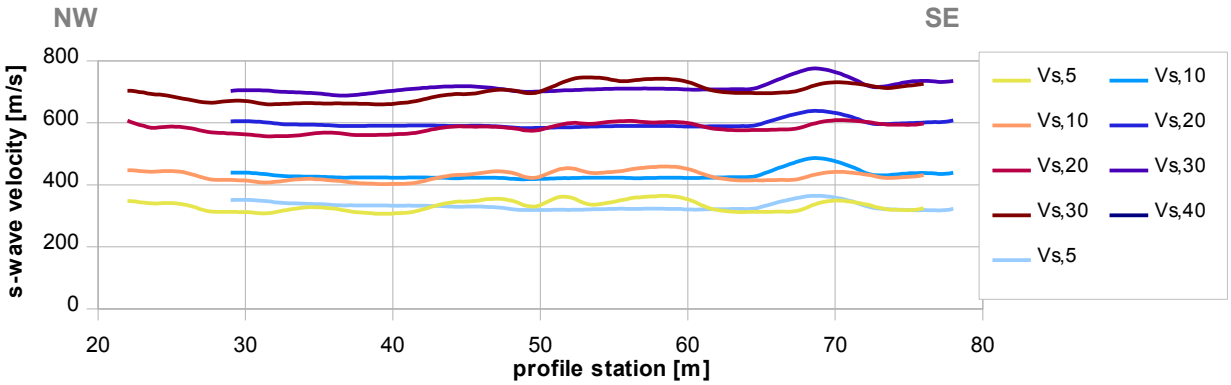

Fig. 3.3l: Graphs of the averaged $v_{s,5}$...-values along the line 09SN_17TORNY-M2 for the PLUS- (blue lines) and MINUS- (red lines) directions.

The average values of the s-wave velocity model $v_{s,5}$, $v_{s,10}$, $v_{s,20}$, $v_{s,30}$, $v_{s,40}$, $v_{s,50}$, $v_{s,100}$ (= average shear wave velocity from the surface to depths of 5 m, … until 100 m) on the line segment nearest to the SED station (Tab. 3.3d) are summarized below:

	Vs,5	Vs,10	Vs,20	Vs,30	Vs,40	Vs,50
MINUS	373	413	536	659	708	n/a
PLUS	384	421	541	671	737	n/a
MEAN	378	417	538	665	722	n/a

	Vs,5	Vs,10	Vs,20	Vs,30	Vs,40	Vs,50
MINUS	332	428	583	699	n/a	n/a
PLUS	329	424	591	709	n/a	n/a
MEAN	330	426	587	704	n/a	n/a

Tab. 3.3d: The average shear wave velocities within the depth intervals from surface down to 5 m, etc.… to 50 m, calculated overall of the line.

3.4 Hybrid Seismic Data Processing

3.4.1 p-wave *Reflection* Seismic Processing Sequence

A) Data conditioning

A1 Reformatting and quality verification of field data
A2 Recording geometry assignment
A3 Data editing (suppression of bad / dead traces, etc.)
A4 Preliminary analysis of refraction velocities

B Filtering and deconvolution

B1 Analytical muting of refraction arrivals
B2 Amplitude recovery / amplitude equalization in time and frequency domains
B3 Predictive deconvolution parameter tests / application
B4 Determination of band limiting corner frequencies / application
B5 Optional 2-D filtering

C) Velocity analysis and stack

C1 Common Depth Point (CDP) sort
C2 Semblance velocity analysis using supergathers of 3 - 5 CDP's
C3 Optional dip move-out correction
C4 Normal Move-Out (NMO) correction and application of stretch mute
C5 Band-pass filtering
C6 CDP stack
C7 Optional coherency filtering

D) Time-depth conversion

D1 Optional spiking deconvolution
D2 Band-pass filtering
D3 Depth conversion
D4 Final display of seismic depth section with inversed polarity (non-SEG-convention)

3.4.2 The presentation of reflection seismic data

The data in a reflection seismic section are presented as an assembly of individual seismic signals at regular intervals along a seismic profile. The simplest way of representing the signals are single wiggle lines (first to the left in the illustration below). A more capturing presentation is the variable area form (second to the left). Combining these two modes results in the var-wiggle mode. Another method of data visualization is the variable density mode (second from the right).

The compressional phase of seismic signals is defined in this report as the onset of the positive amplitude excursion in black (Fig. 3.4a). Since the source signal is produced by an explosion or by an impact at the surface, the signal starts off with a compression of the ground particles. Thus the arrivals of reflection events are defined by the compressional phase.

In rare situations of velocity inversions, cases in which formation velocities are lower than in the layers above, polarity reversals of the reflected signals occur. The beginning of the reflection event would then be characterized by a dilatational phase, represented in this report as a negative amplitude excursion, i.e. in white.

The final p-wave seismic depth sections are displayed in Fig. 3.4b and 3.4c, the hybrid sections in Fig. 3.4j and -k further below.

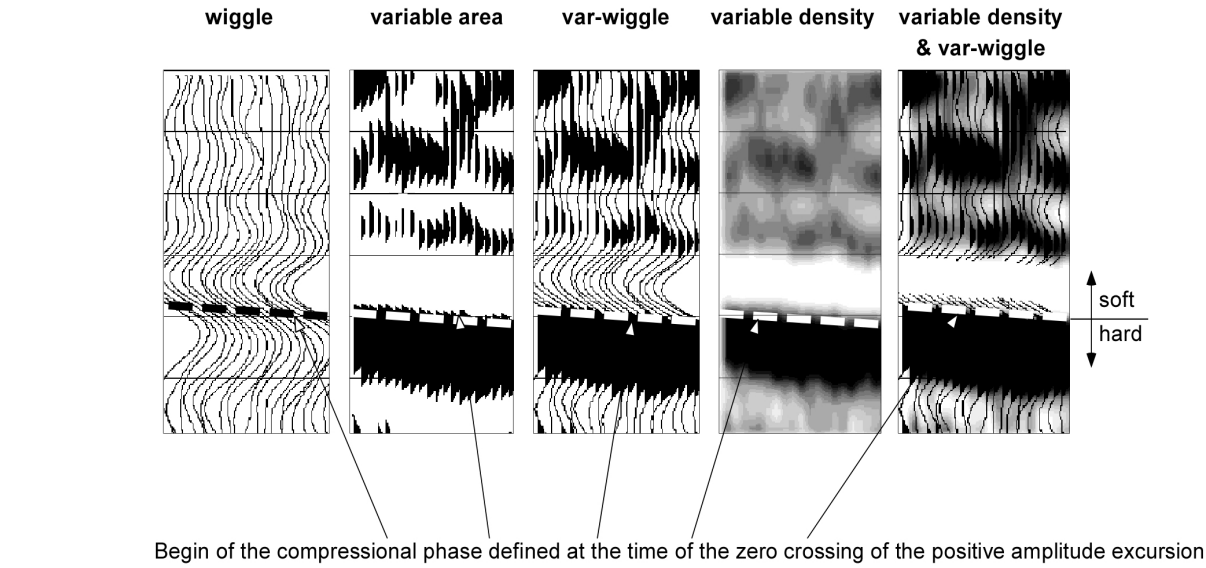

Fig. 3.4a Representation of reflection seismic data and the definition of a reflection event.

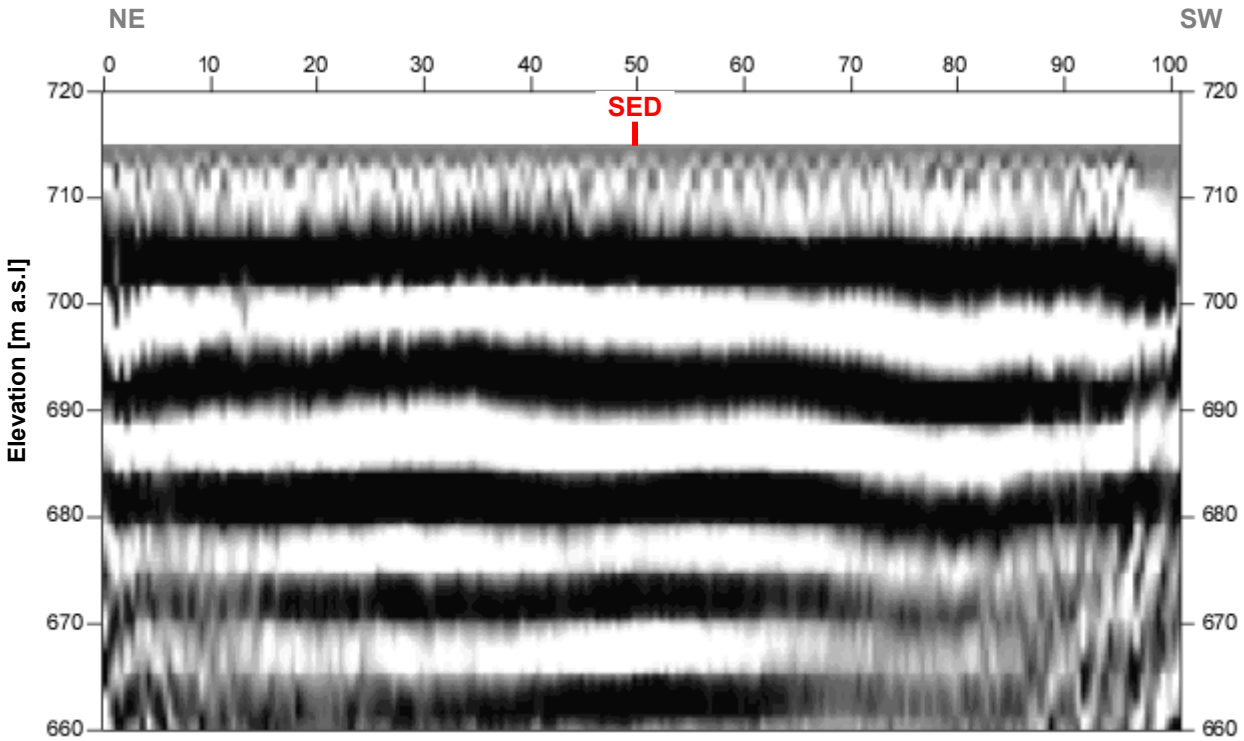

Fig. 3.4b: Seismic depth section of line 09SN_17TORNY-P1 with variable density mode presentation. Vertical axis: elevation [m a.s.l.], horizontal axis: profile meter; no vertical exaggeration. The station spacing is 1 m.

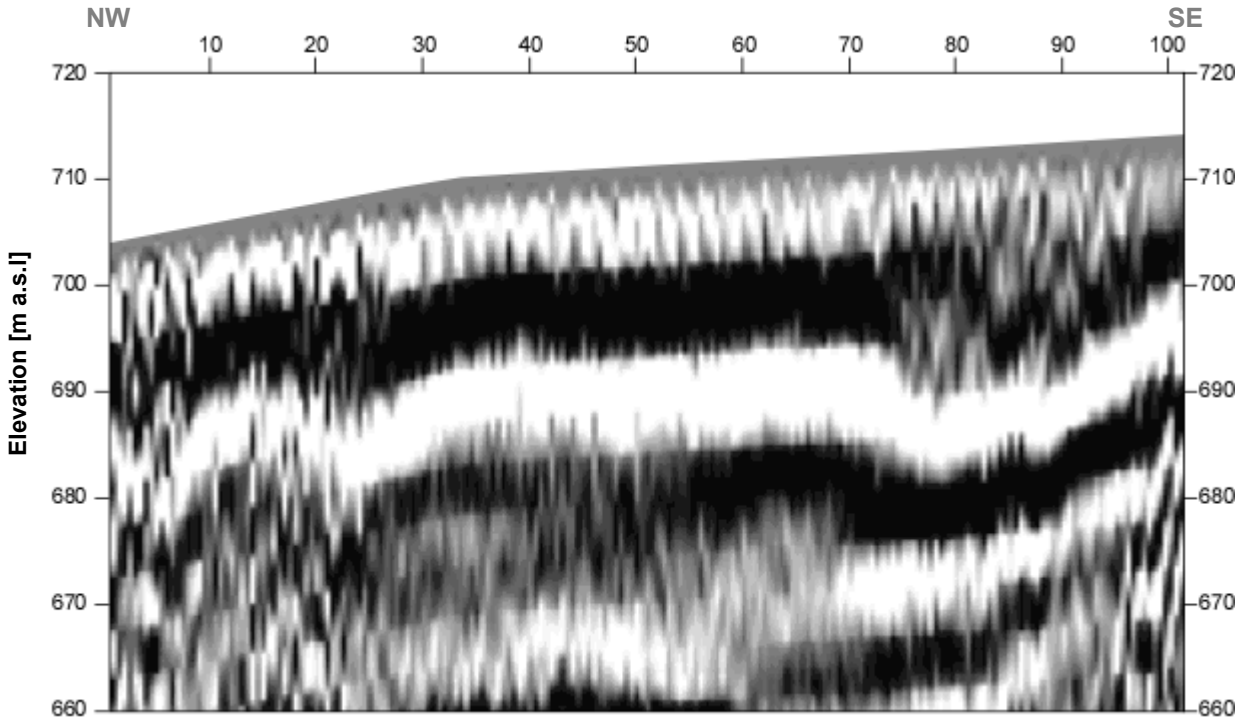

Fig. 3.4c: Seismic depth section of seismic line 09SN_17TORNY-P2 with variable density mode presentation. Vertical axis: elevation [m a.s.l.], horizontal axis: profile meter; no vertical exaggeration. The station spacing is 1 m.

3.4.3 p-wave refraction tomography processing

The seismic p-wave refraction processing steps are analogous to those described in paragraph 3.2. For a detailed method statement and a description of the processing steps please refer to the summary report. The Figs. 3.4d to 3.4i and Tab. 3.4a illustrate the intermediate processing steps and the final result.

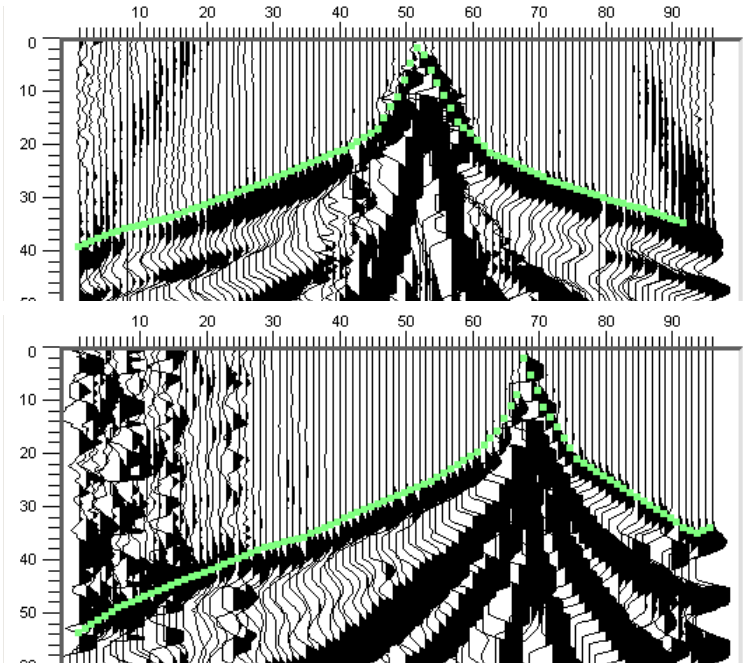

Fig. 3.4d: p-wave records from 09SN_17TORNY-P1 (above) and -P2 (below) with positive amplitude excursions in black. Colored dots mark the manually picked first break arrival times. Vertical axis: travel time in ms, horizontal axis: station numbers spaced at 1 m.

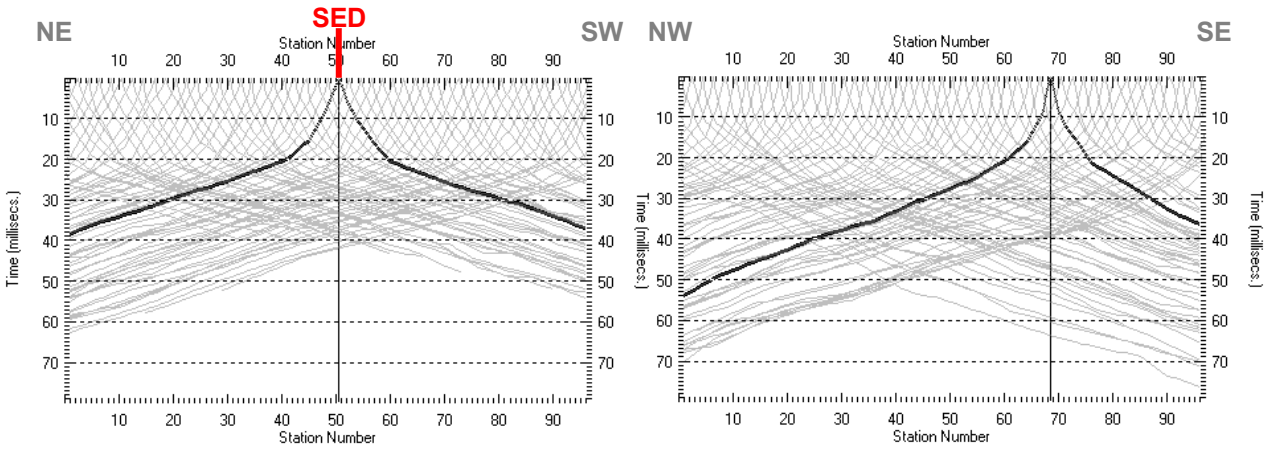

Fig. 3.4e: Travel time curves of p-wave arrival time picks from line 09SN_17TORNY-P1 (left) and -P2 (right). Vertical axes: travel time [ms], horizontal axes: station number (= profile meter).

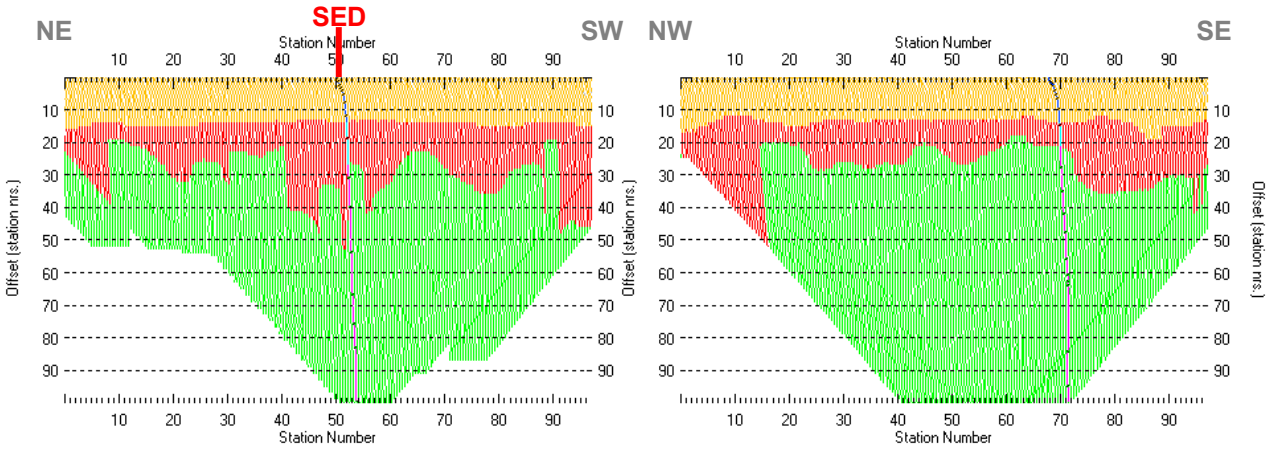

Fig. 3.4f: 3-dimensional distance-travel time diagrams at the mid-points between source points and receiver stations are instrumental when using the analytical CMP derivation of the initial velocity field. The horizontal axes are along the CMP positions and the travel time respectively, the vertical axis denotes the offset distance between source and receiver positions.

Depth [m]	Vp [m/s]
0.2	302
0.5	401
0.8	448
1.3	510
2.0	614
2.9	768
3.9	994
5.2	1345
7.1	1849
9.4	2344
12.5	2907
16.4	3079
21.4	3523
28.0	3907
36.6	3865

Depth [m]	Vp [m/s]
0.0	232
0.5	304
0.8	377
1.3	497
2.0	667
2.8	868
3.8	1082
5.2	1318
7.0	1636
9.3	1997
12.3	2294
16.1	2488
21.1	2937
27.6	3183
36.1	3390
47.1	3628

Tab. 3.4a: Initial 1D p-wave velocity model derived from real data (left: 09SN_17TORNY-P1; right: -P2).

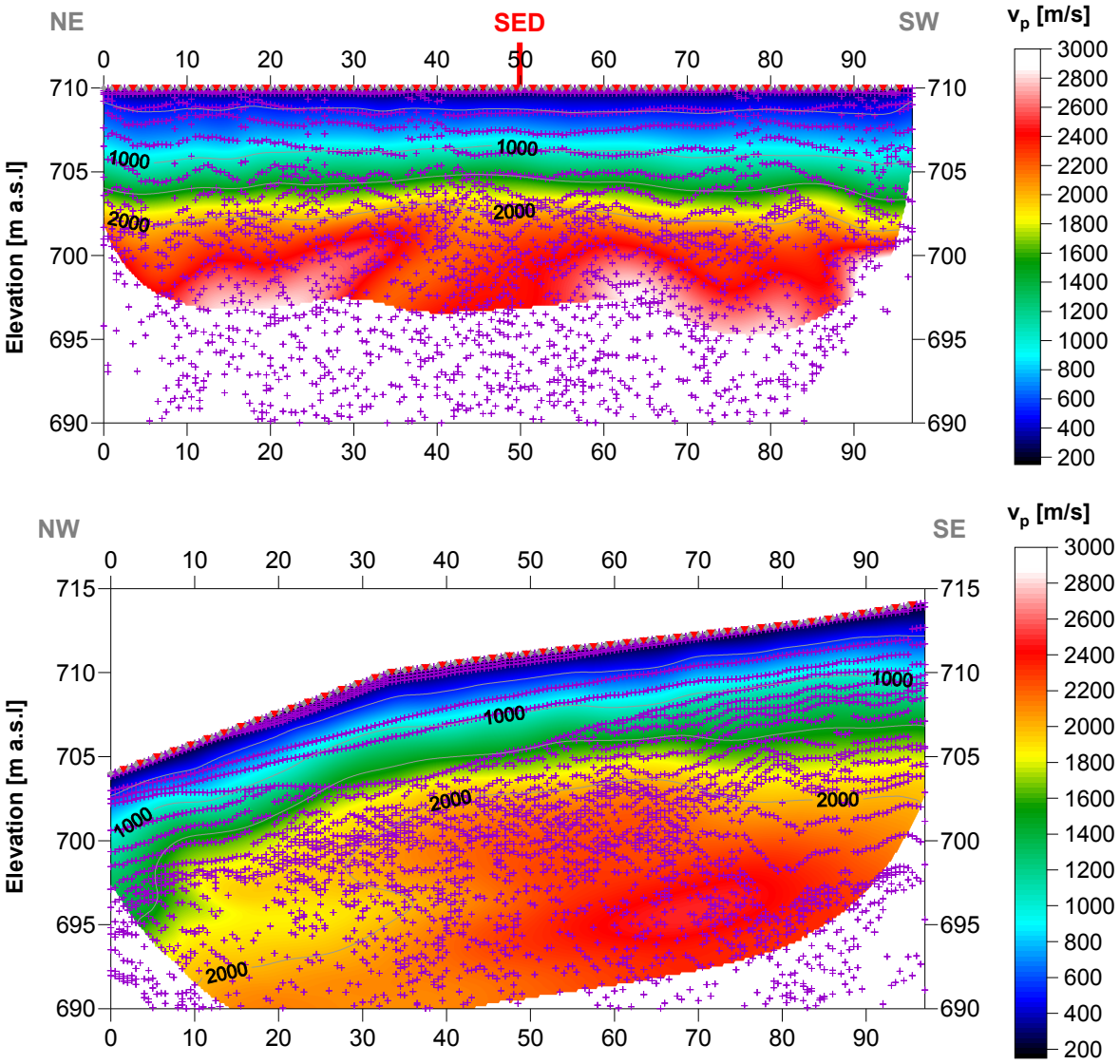

Fig. 3.4g: Compressional wave velocity field image along the seismic profiles 09SN-17TORNY-P1 (above) and -P2 (below). Red/white colors indicate solid rock, blue/black colors unconsolidated sediments and soil. Vertical axis: elevation [m a.s.l]; horizontal axis: profile meter; color scale: v_s [m/s]; vertical exaggeration: 2:1; gray squares: receiver stations; red triangles: shot positions; magenta crosses: positions of determined velocity values.

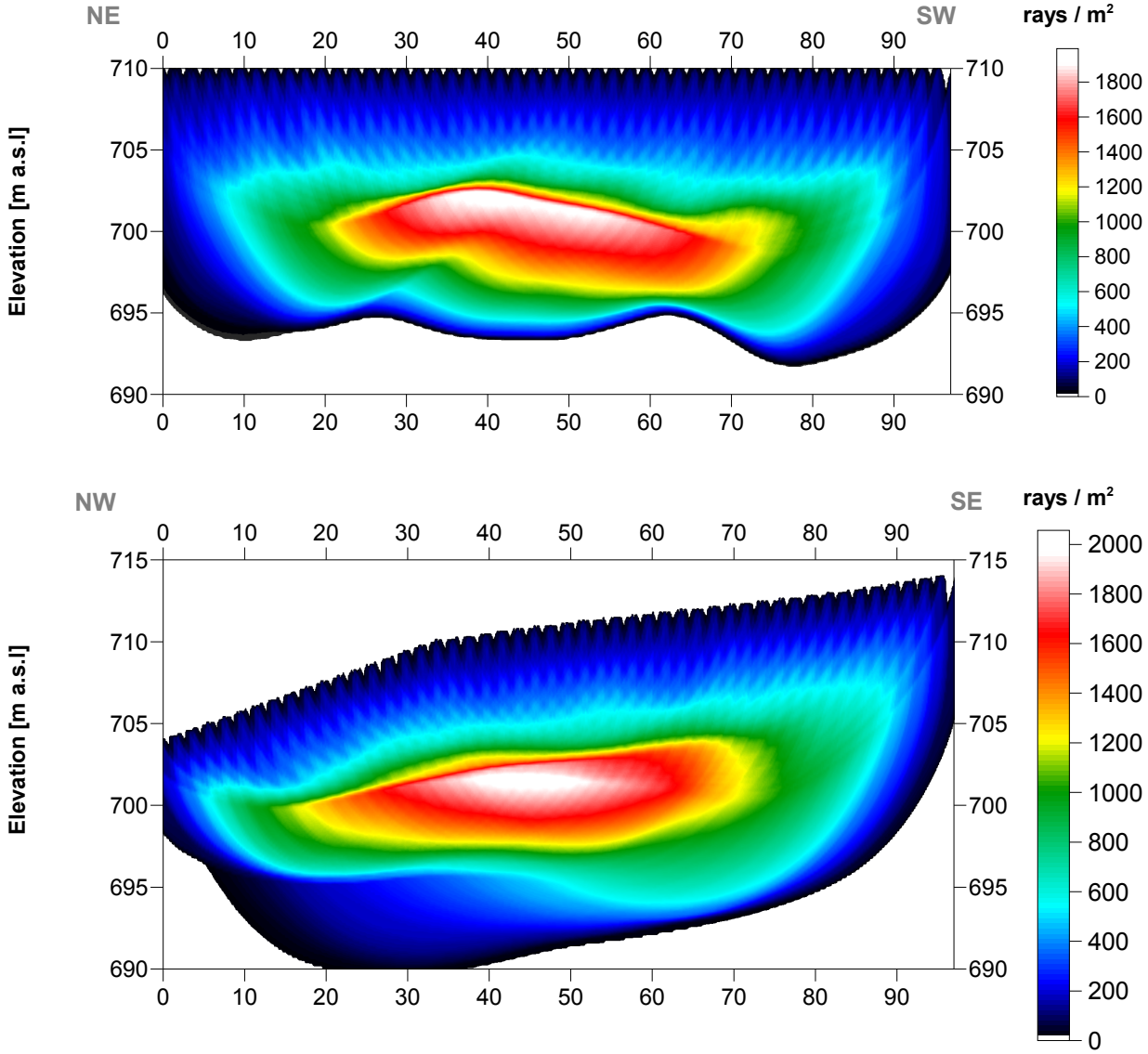

Fig. 3.4h Compressional wave subsurface ray path density along the seismic line 09SN_17TORNY-P1 (above) and -P2 (below). Red/white colors indicate high velocity contrast between two layers, blue/black colors low coverage areas. Vertical axis: elevation [m a.s.l]; horizontal axis: profile meter; color scale: ray paths per m²; vertical exaggeration: 2:1.

Depth [m]	Vp [m/s]
0.0	250
1.2	479
2.2	640
3.2	834
4.2	1069
5.2	1339
6.2	1620
7.2	1888
8.3	2120
9.3	2297
10.3	2425
11.3	2492
12.3	2551
13.3	2556
14.3	2771

Depth [m]	Vp [m/s]
0.0	205
1.4	475
2.7	803
4.1	1110
5.4	1385
6.8	1634
8.1	1829
9.5	1972
10.8	2053
12.2	2098
13.5	2137
14.9	2201
16.2	2275
17.4	2284
18.8	2240
20.1	2183

Tab. 3.4b: Final 1D p-wave velocity model derived from real data at line 09SN_17TORNY-P1 (left) resp. line 09SN_17TORNY-P2 (right) .

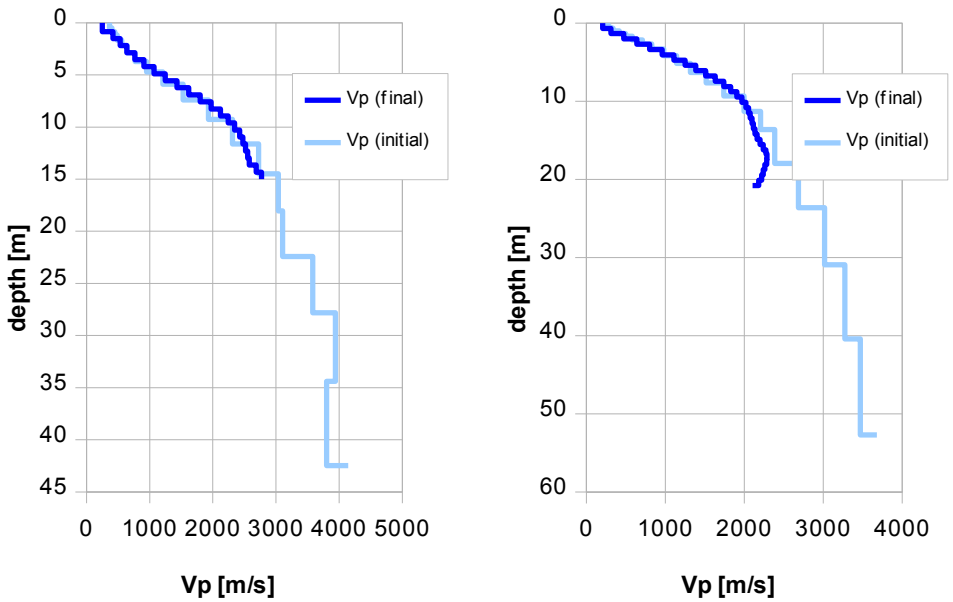

Fig. 3.4i: Final 1D p-wave velocity model derived from real data at line 09SN_17TORNY-P1 (left) resp. line 09SN_17TORNY-P2 (right). Initial 1D p-wave velocity model values are given in Tab. 3.4a.

3.4.4 Representation of the hybrid seismic section

The hybrid seismic section is the reflection seismic section with the superimposed p-wave velocity field. It portrays the geological structures and the p-wave velocity field, the latter being indicative for the rock / soil rigidity. The uninterpreted hybrid seismic section is portrayed in Fig. 3.4j and 3.4k below.

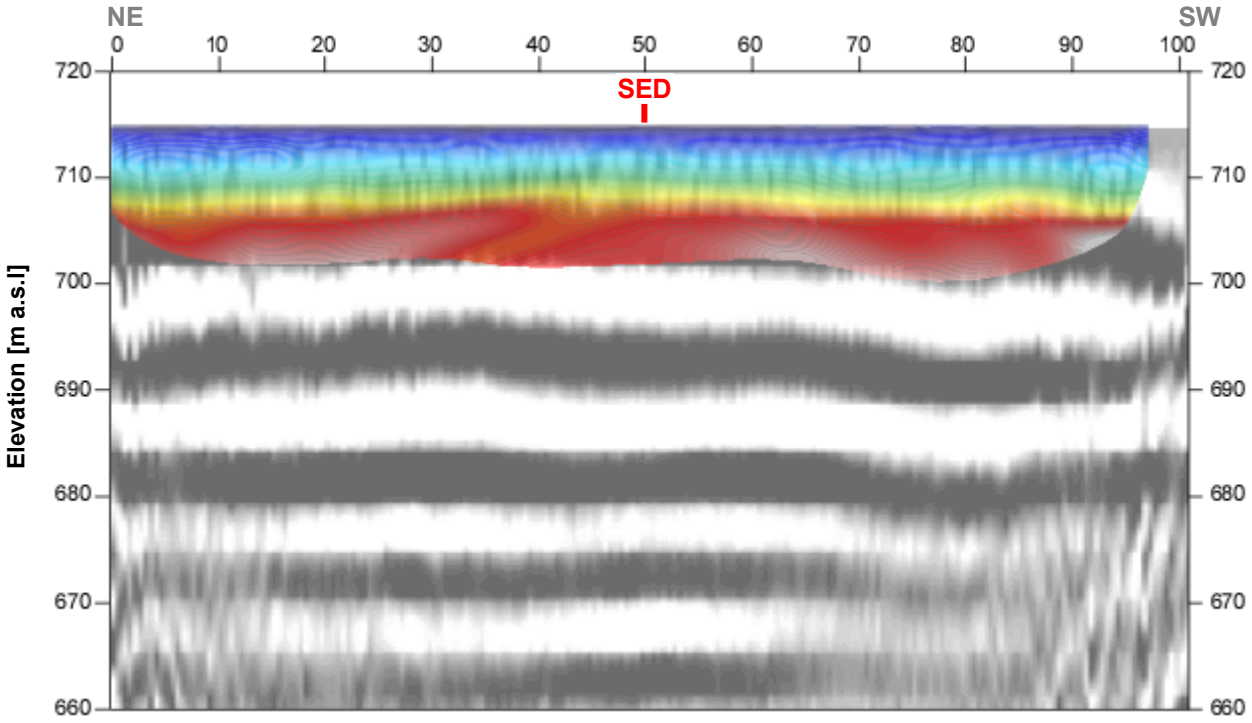

Fig. 3.4j Uninterpreted hybrid seismic section 09SN_17TORNY-P1: superimposed onto the seismic reflection section is the color encoded p-velocity field derived by refraction tomography (no vertical exaggeration).

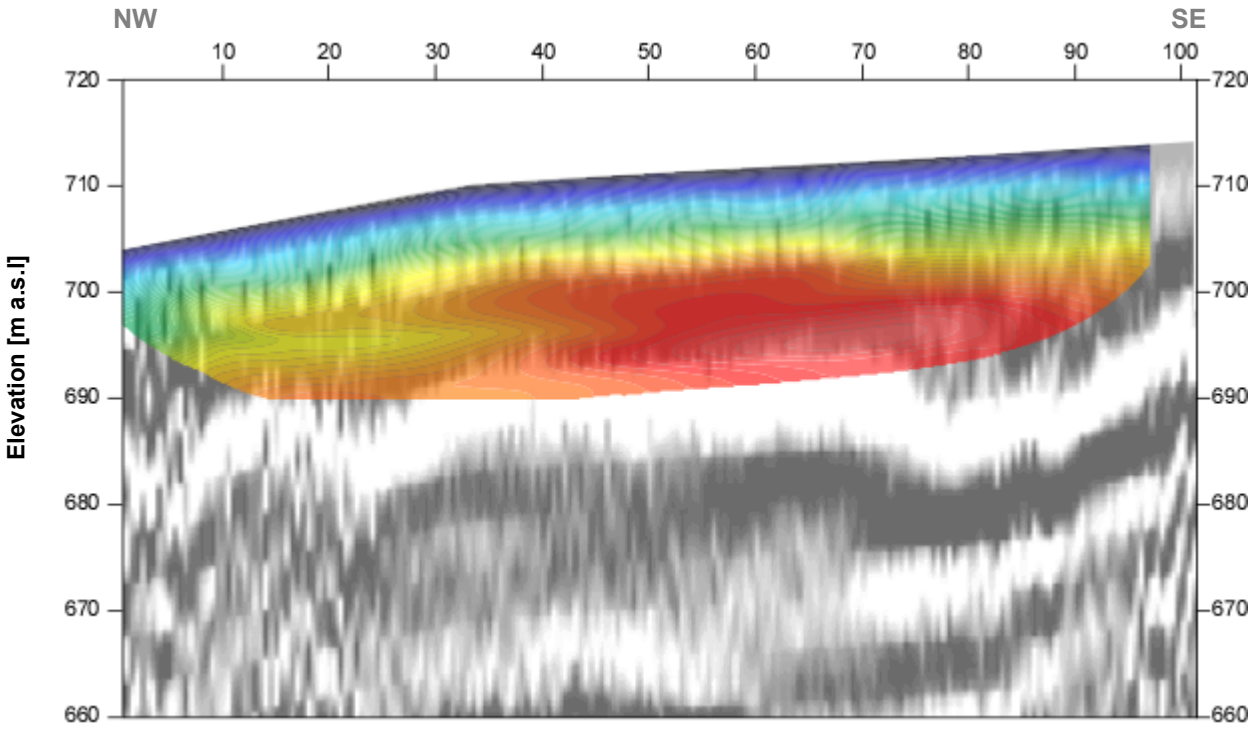

Fig. 3.4k Uninterpreted hybrid seismic section 09SN_17TORNY-P2: superimposed onto the seismic reflection section is the color encoded p-velocity field derived by refraction tomography (no vertical exaggeration).

4 DISCUSSION OF THE RESULTS

4.1 Summary and Validation of the Results

Compressional and shear wave velocity data from refraction seismic surveys both p-wave and s-wave and also the MASW survey data from profiles 09SN_17TORNY-1 and 09SN_17TORNY-2 are shown in Tab. 4.1 for the uppermost 30 m.

Depth	Vp1	Vp2	Vs1	Vs1	Vs2	Vs2	Vs1	Vs2
	refract	refract	refract	calc	refract	calc	MASW	MASW
0	250	205		144	122	119		
1	418	311	394	241	177	180	514	399
2	532	640	305	307	265	369		197
3	640	803	244	369	435	463	408	433
4	908	960	290	524	504	554	296	
5	1247	1252	362	720	588	723		
6	1433	1385	456	827	614	800	448	561
7	1802	1634	564	1040	680	944		
8	1973	1740	665	1139	773	1005		591
9	2243	1906	741	1295	883	1100	599	
10	2345	1972	802	1354	938	1139		
11	2475	2053	860	1429	1050	1185		743
12	2518	2077	916	1454	1098	1199		
13	2551	2117	943	1473	1163	1222	656	
14	2687	2137	949	1551	1255	1234		
15	2771	2201	943	1600	1291	1271		941
16		2241	948		1258	1294		
17		2289	955		1282	1321	789	
18		2284	958		1212	1319		
19		2240				1294		
20		2220	958			1282		1111
21		2106	975			1216		
22			992				1134	
23			1007					
24			1036					
25			1064					
26			1097					1144
27			1137					
28			1170					
29			1191				1348	
30			1208					
31			1228					
32			1254					1265
33			1282					
34			1303					
35								
36							1176	

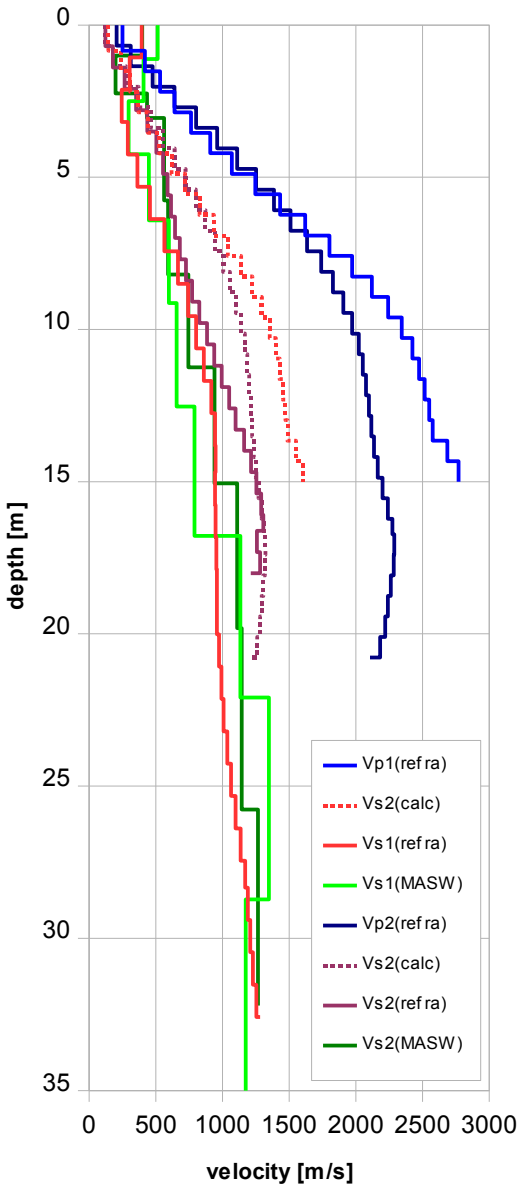

Tab. 4.1: Shear and compressional wave velocity model determined at the SED station TORNY.

Fig. 4.1: Graphic display of shear (continuous lines) and compressional (dotted lines) wave velocities determined at the SED station. In green colors values from line 09SN_17TORNY-1 and in blue values from line 09SN_17TORNY-2. at the SED station.

4.2 Validation of the methods and their results

Due to methodological differences, v_s velocities derived by MASW analysis and by the refraction tomography technique may differ considerably. This is because MASW analysis cannot image small rock/soil inhomogeneities as a dispersion image with an array length of i.e. 40-m only yields one single v_s-value at each depth. On the other hand, refraction diving wave tomography results produce v_s-sections with a high lateral resolution, but fail to provide information at greater depths.

4.3 Error Estimates

The error estimates given in Tab. 4.3 below are relevant only in the context of this survey.

Surveying method	Type of result	Error estimate
v_s – refraction tomography	v_s – velocity field image	10%
MASW only "+" or only "-" values*	v_s – velocity field image	15%
MASW (mean of "+" & "-" values)*	v_s – velocity field image	10%
v_p – refraction tomography	v_p – velocity field image	8%
Reflection seismic surveying	Image of subsurface structures	n.a.

** MASW values in the uppermost 4 m are prone to an error of about 20 % (only one direction) resp. 10 % (mean of both directions).*

Tab. 4.2 Error estimates for the methods applied. Note that higher error estimates are to be taken into account with increasing depths.

The above error estimates are of a qualitative character only. Due to very high quality seismic data with a hight content of surface wave energy, all the derived v_s- and v_p-values seems to be of high precision. All velocity data coincide very well, independently from the methodological differences.

At the SED station TORNY (Torny-le-Grand FR), the refraction velocity images both from shear and compressional wave analysis show coincident structures. The MASW figures are in the same range as the values obtained from the shear wave diving wave refraction tomography surveys.

4.4 The Geophysical Interpretation

The most conclusive information about the subsurface structures is provided by the results of the hybrid seismic section (v_p-refraction tomography profiling and reflection seismic section) and confirmed by the evaluation results of the v_s-refraction tomography data.

As can be seen from the v_s and v_p refraction tomography sections in Fig. 3.2e/f & Fig. 3.4g/h, the topography of the bedrock surface is imaged well on both profiles. The geological interpretation of the seismic events is shown in Fig. 4.2a. The rock surface is to find in a depth of about 8 m with humble undulations. A nearly planar layering is visible over all of the section. No any tectonic fault could be found on profile 09SN_17TORNY-P1.

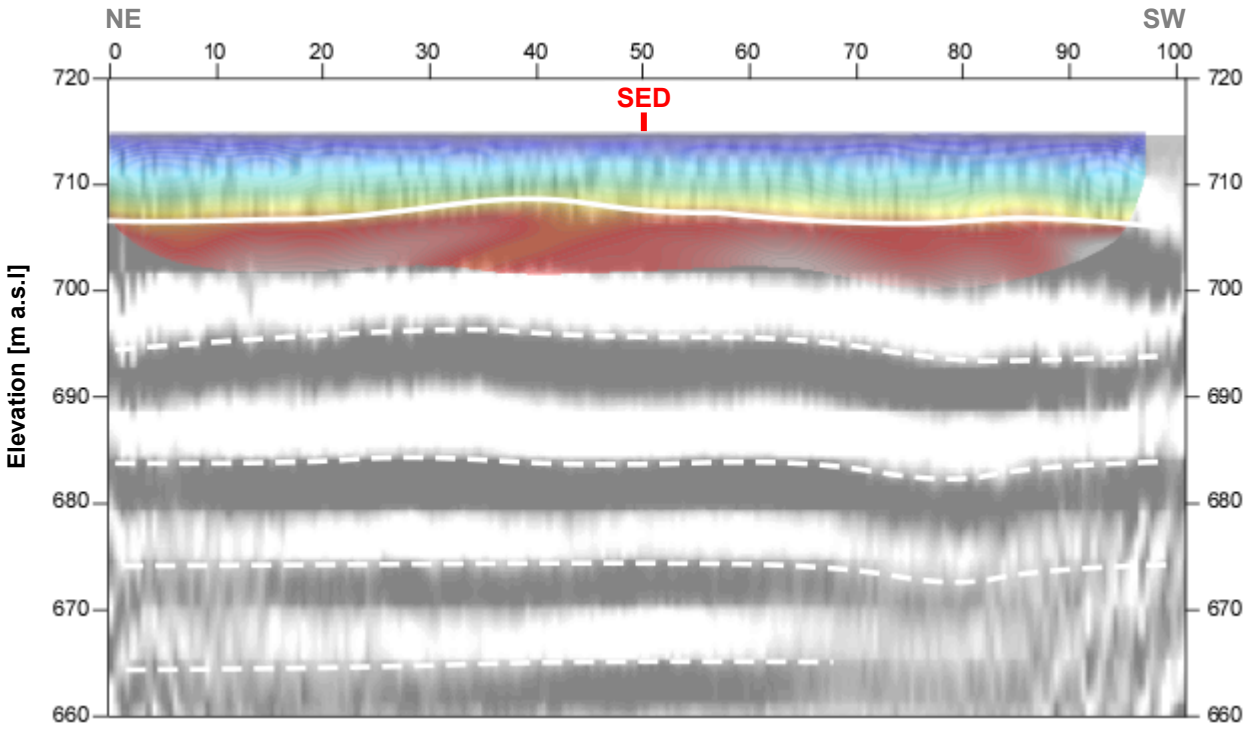

Fig. 4.2a Geophysical interpretation of the hybrid seismic section 09SN_17TORNY-P1. White lines denote layer boundaries, continuous line the bedrock surface.

The geological interpretation of the seismic events of line 09SN_17TORNY-2 is shown in Fig. 4.2b. The topography of the bedrock surface is nearly sub-parallel to the topography. In the Southeast a marginal depression is imaged, concordant to a assumed tectonic fault in the underlaying bedrock (upper marine molasse).

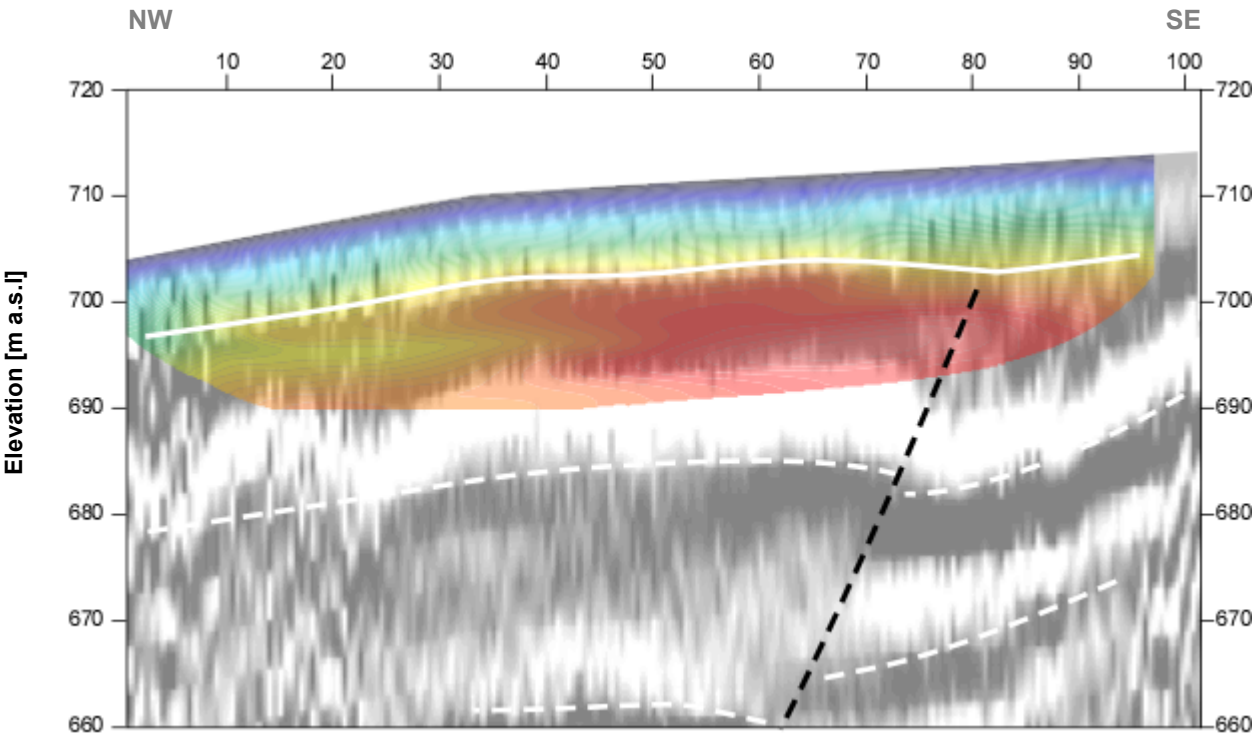

Fig. 4.2b Geophysical interpretation of the hybrid seismic section 09SN_17TORNY-P2. White lines denote layer boundaries, the continuous one marks the bedrock surface; black dotted lines are indicative of suspected faulting with a wide loosening zone (black hatched area).

5 SUMMARY AND CONCLUSIONS

- In March 2009 a combined seismic s- and p-wave survey was carried out at the SED earthquake monitoring station TORNY (near Torny-le-Grand FR).
- The shear wave data have been evaluated by conventional diving wave refraction tomography techniques in order to derive the s-wave velocity field along the seismic line.
- The p-wave data have been processed
  - firstly to derive a 2D s-wave velocity field by using the MASW (**M**ultichannel **A**nalysis of **S**urface **W**aves) technique;
  - and secondly, according to the hybrid seismic data processing scheme for representing the subsurface structures in a combined reflection seismic section with the superimposed p-wave velocity field.
- The shear wave velocity range determined by the MASW method in the uppermost 30 meters spans from values of 197 m/s to 1348 m/s.
- The scalar values derived by the MASW survey at the SED station (seismic line 09SN_17TORNY-M1, profile station 50; seismic line 09SN_17TORNY-M2, profile station 25, 125 m offset) are the following:

line 1			line 2		
$v_{s,5}$	=	378 m/s	$v_{s,5}$	=	330 m/s
$v_{s,10}$	=	417 m/s	$v_{s,10}$	=	426 m/s
$v_{s,20}$	=	538 m/s	$v_{s,20}$	=	587 m/s
$v_{s,30}$	=	665 m/s	$v_{s,30}$	=	704 m/s
$v_{s,40}$	=	772 m/s	$v_{s,40}$	=	n/a

- The maximum refraction shear wave velocity derived in the uppermost 30 m is 1208 m/s at a depth of 30 m.
- The maximum p-wave velocity determined is 2771 m/s at a depth of 15 m.
- The geophysical interpretation of the subsurface structures in this report are to be validated and incorporated into a comprehensive appraisal by a geologist familiar with the local geological setting.

Schwerzenbach, 20th May 2009

Walter Frei
dipl. Natw. ETH
managing director

Lorenz Keller
dipl. Natw. ETH
project manager